Arabidopsis Mutants Used to Study the Effects of S(+)-Beta-Methyl-alpha, Beta-Diaminopropionic Acid (BMAA), a Cycad-Derived Glutamate Receptor Agonist

by

Nora M. Barboza

A dissertation submitted to the Graduate Faculty in Biology in partial fulfillment of the requirements for the degree of Doctor of Philosophy,

The City University of New York

2004

UMI Number: 3115229

UMI Microform 3115229

ProQuest Information and Learning Company
300 North Zeeb Road
P.O. Box 1346
Ann Arbor, MI 48106-1346

This manuscript has been read and accepted for the Graduate Faculty in Biology in satisfaction of the dissertation requirement for the degree of Doctor of Philosophy.

Jan. 26, 2004
Date

Chair of Examining Committee
Dr. Dennis Stevenson, New York Botanical Garden

January 28, 2004
Date

Executive Officer
Dr. Richard L. Chappell

Dr. Dwight Kincaid, Lehman College

Dr. . Miguel Cervantes-Cervantes, Lehman College

Dr. Timothy Short, Queens College

Dr. Gloria Coruzzi, New York University

Supervising Committee

The City University of New York

ABSTRACT

Arabidopsis Mutants Used to Study the Effects of S(+)-Beta-Methyl-alpha, Beta-Diaminopropionic Acid (BMAA), a Cycad-Derived Glutamate Receptor Agonist

by

Nora M. Barboza

Advisors: Dr. Dennis Wm. Stevenson at the New York Botanical Garden and Dr. Gloria M. Coruzzi at New York University

To begin to understand the molecular mechanisms that regulate plant glutamate receptors, a forward genetic approach to isolate mutants resistant to the effects of BMAA, an animal glutamate receptor agonist, was developed. Because of the neurotoxic properties attributed to BMAA on the animal iGluRs, characterization of these mutants may provide new insights into the general functioning of glutamate receptors. BMAA affects *Arabidopsis* seedlings by inducing elongation of the hypocotyl. But BMAA insensitive (*bim*) mutants are resistant to BMAA and have short hypocotyls. The *bim* mutants were subgrouped into three Classes, based on their dark-grown morphology: Class I *bim* mutants have an etiolated phenotype, Class II *bim* mutants have short hypocotyls and closed cotyledons, and Class III *bim* mutants are constitutively photomorphogenic with short hypocotyls and open cotyledons. This study focuses on three *bim* mutants from Class II. The identity of the mutants was revealed through positional cloning, genetic complementation analysis, and gene sequencing. Positional cloning identified *CHITINASE-LIKE* gene (*CTL*1) and genetic

complementation identified *PROCUSTE* (*PRC*1). The inability of these mutants to elongate their hypocotyl is likely due to cell wall defects. In order to understand the link between these cell wall mutants and BMAA effects, transcript levels for the identified genes were quantified under different conditions. *PROCUSTE* and *CHITINASE-LIKE* genes were found to be repressed by light, but when BMAA is added there is a slight induction. In the dark, the presence of BMAA causes a significant repression of the transcript levels when compared to those in the absence of BMAA. I provide a model to describe the effect of BMAA on PRC1 and CTL1 in wild type. A separate series of experiments described in the last chapter provides data indicating that BMAA may alter ion sensitivity in wild-type *Arabidopsis* seedlings.

ACKNOWLEDGEMENTS

I would like to thank my dissertation advisor Dr. Gloria M. Coruzzi for her guidance and support. I am grateful to Dr. Coruzzi for allowing me to conduct my research in her lab and to be part of her excellent research and learn from her deep knowledge of molecular biology. I wish to thank Dr. Dennis Wm. Stevenson, my CUNY advisor for his support and enthusiasm. I would like to express my appreciation to Dr. Dwight Kincaid, not only for supporting me as a graduate student but also for his efforts to maintain a high-quality education at CUNY in a supportive environment, as well as for his commitment to and encouragement of his students. I like to thank Dr. Miguel Cervantes for encouraging me to obtain a Ph.D. in molecular biology and for all his scientific help. I am grateful to Dr. Timothy Short, a member of my committee, for his help and scientific input.

I would like to express my gratitude to members of the Benfey and Coruzzi labs for providing a stimulating and pleasant environment in which to work. I obtained a great deal of my present knowledge in molecular biology thanks to their mentoring and patience. Many thanks to Alex Clark, Alexis Cruikshank, Andrei Kouranov, Joanna Chiu, Karen Thum, Laurence LeJay, Peter Palenchar, Suzan Runko and Trevor Strokes; to Michael Shin, Eric Brenner, and Anita Fernandez for helpful discussions and critical comments on the manuscript; to Alice Paquette, Tal Nawy, and Kenneth Birnbaum for their numerous scientific discussions; to Gary Schindelman and François Roudier for teaching me all about gene mapping. Thanks to our lab manager Maria Shamis for

promptly ordering my reagents. Thanks also to Dr. Gail Smith and Dr. Claude Brathwaite from the City University of New York for their encouragement and support and for helping me find financial support over the years as a graduate student. This work was supported in part by a grant from the National Institute of Health – special thanks to Anthony René for his administrative help in processing the fellowship.

TABLE OF CONTENTS

Abstract of the dissertation iii

Acknowledgments v

Table of contents vii

List of tables x

List of figures xi

List of Abbreviations xiv

Chapter 1 1

General Introduction

Animal glutamate receptors 2

Glutamate receptors in Arabidopsis 3

Glutamate gating in plants 3

Evidence for the presence of glutamate receptors in plants 4

Predicted function of GLRs in *Arabidopsis*. 5

BMAA a glutamate receptor agonist 6

Neurotoxic properties of BMAA 6

BMAA activates intracellular Ca^{2+} in animals 7

Theme of the thesis 8

Figures 10

Chapter 2 13

Arabidopsis Mutants Resistant to S(+)-β-Methyl-α, β-Diaminopropionic

Acid, a Cycad-Derived Glutamate Receptor Agonist

Abstract 14

Introduction 15

Results 16

Discussion 20

Materials and Methods 23

Figures and Tables 25

Chapter 3 32

Genetic Complementation of the *bim* Mutants and Positional Cloning of *bim*4, a Class II BMAA-Insensitive Mutant

Abstract 33

Introduction 34

Results 36

Discussion 42

Materials and Methods 46

Figures and Tables 51

Appendix to Chapter 3 59

Chapter 4 80

BMAA May Alter Ion Sensitivity in *Arabidopsis* Seedlings

Abstract 81

Introduction 82

Results 84

Discussion 85

Materials and Methods 87

Figures 89

References 97

List of tables

Chapter 3:

Table 3.1. Genotype and phenotype of the 10 isolated *bim* mutants 52

Appendix to Chapter 3:

Table A-3.1 Introgressed plants used to create a new mapping population to achieve the mapping of *BIM4* 59

Table A-3.2. Statistical summary of transcript levels of *BIM3* (*PRC*) after a 10 hr treatment 73

Table A-3.3. Statistical summary of transcript levels of *BIM4* (*CTL*) after a 10 hr treatment 74

Table A-3.4. Statistical summary of hypocotyl length in absence (MS) and presence (BMAA) of BMAA after 3, 4, 5, 6, and 7 days of dark-grown treatment.. 75

Table A-3.5. Statistical summary of hypocotyl length in absence (MS) and presence (BMAA) of BMAA after 3, 4, 5, 6, and 7 days of light-grown treatment.. 76

Table A-3.6. Preliminary ANOVA of the dependent variable. 77

Table A-3.7. Significant test of slope variation. 78

Table A-3.8. Final ANCOVA table. 79

List of figures

Chapter 1:

1.1. Schematic of a glutamate receptor subunit. 10

1.2. Transmission at a chemical synapse. 11

1.3. Chemical structure of glutamate and BMAA. 12

Chapter 2:

2.1. Effect of BMAA on *Arabidopsis* seedlings. 25

2.2. Genetic screen to isolate BMAA insensitive morphology (*bim*) mutants. 26

2.3. *bim* mutants are insensitive to BMAA. 27

2.4. Quantification of the hypocotyl length of *bim* mutants grown in the light in the presence and absence of BMAA 28

2.5. *bim* mutants fall into three separate classes based on their dark-grown morphology. 29

2.6. Two representative *bim* mutants resistant to iGluR agonist BMAA 30

2.7. Quantification of the hypocotyl length of *bim* mutants grown in the dark in the presence and absence of BMAA. 31

Chapter 3:

3.1. Quantification of hypocotyl length of wild-type seedlings grown in light or in the dark in the presence or absence of 50μM BMAA. 52

3.2. Positional cloning of the *BIM4* locus. 53

3.3. Phenotypic analysis of *bim3* and *bim4* mutants. 54

3.4. Effect of BMAA on cross sections of light and dark-grown hypocotyl of wild type compared to *bim3* and *bim4* mutants. 55

3.5. Quantification of gene expression of *BIM3* (*PRC*) (A) and *BIM4* (*CTL*) (B) in the presence and absence of BMAA in wild-type seedlings 56

3.6. In the dark BMAA partially mimics light on a subset of genes 57

3.7. A proposed model representing the effect of BMAA on *BIM3* (*PRC*) and *BIM4*(*CTL*).....58

Appendix to Chapter 3:

A-3.1. SSLP and CAPS markers designed to map *bim4*.....65

A-3.2. F2 informative recombinants used to fine map *bim4*.....68

A-3.3. Genes in BAC T20M3.....69

A-3.4. Genomic sequence of the *AtCTL1*.....70

A-3.5. Curve analysis for *PRC, CTL* and *eIF4A*.....71

A-3.6. LightCycler analysis setting report.....72

Chapter 4:

4.1 Quantification of light-grown hypocotyls in NaCl or KCl in the absence and presence of BMAA 89

4-2. Effect of BMAA on one week-old *Arabidopsis* seedlings grown on increasing concentrations of NaCl.....90

4.3. Effect of BMAA on one week-old *Arabidopsis* seedlings grown on increasing concentrations of KCl.....91

4.4. Effect of BMAA in two week-old light-grown *Arabidopsis* seedlings on high concentrations of NaCl 92

4.5. Effect of BMAA in two week-old light-grown *Arabidopsis* seedling on high concentrations of KCl.....93

4.6. Comparison of the effect of BMAA on two week-old *Arabidopsis* seedlings on high concentrations of NaCl or KCl. 94

4.7. The opposite effect of Na^+ and K^+ on *Arabidopsis* seedlings is reversed by BMAA. 95

List of Abbreviations

AMPA	α-amino-3-hydroxy-5-methylisoxazole-4-propionic acid
bim	BMAA insensitive morphology
BMAA	S(+)-β-methyl-α, β-diaminopropionic acid
CAPS	Cleaved Amplified Polymorphic Sequence
CTL	CHITIN-LIKE
DNQX	6,7-dinotroquinoxaline-2,3-(1H, 4H)-dione
ELP	ectopic lignin deposition on pith
EMS	ethyl methane sulfonate
iGluRs	ionotropic glutamate receptors
iGLRs	Plant ionotropic glutamate receptors
INDELs	Insertion Deletions
NMDA	N-methyl-D-Aspartate
PRC	PROCUSTE
SNP	Single Nucleotide Polymorphism
SSLP	Simple Sequence Length Polymorphism
TAIR	The Arabidopsis Information Resource
VSP	Vegetative Storage Protein

Chapter 1

General Introduction

Animal glutamate receptors

Glutamate (Glu) is the predominant excitatory neurotransmitter in the brain and activates glutamate receptors (GluR) at the post-synaptic membrane (Gasic and Hollman, 1992; Hollman and Heinemann, 1994) (Fig. 1.1). As such it is involved in almost all aspects of the function of the central nervous system, including sensing environmental cues and memory (Maren and Baudry, 1995; Asztely and Gustafsson, 1996). One subgroup of GluRs is composed of the ionotropic GluRs, which function as Glu-gated ion channels that convey rapid synaptic transmission (Nakanishi, 1992; Wisden and Seeburg, 1993). In animals, iGluRs are pharmacologically classified into subgroups, each defined by selective activation by different glutamate agonists: N-methyl-D-aspartate (NMDA), a-amino-3-hydroxy-5-methylisoxazole-4-propionic acid (AMPA), and kainate (MacDermott, 1987; Dingledine et al., 1999).

iGluRs are Na^+ and/or Ca^{2+} permeable channels. Non-NMDA iGluRs are Na^+ permeable channels that open upon binding of the neurotransmitter and rapidly desensitize. NMDA iGluRs have a delayed opening. If depolarization continues to persist because of the non-NMDA iGluRs, then NMDA iGluRs open to release Na^+ and Ca^{2+} and initiate signaling processes (Mayer et al., 1995). A unique feature of NMDA receptors for efficient gating is their requirement for binding both glutamate and glycine as a co-agonist (Johnson and Ascher, 1987; Kleckner and Dingledine, 1988). NMDA iGluR are interesting for at least two reasons: the Ca^{2+} influx may activate other Ca^{2+} dependent pathways (Favaron et al., 1990; Nichols et al., 1990; Williams et al., 1989) and Ca^{2+} influx may be responsible for an imbalance of a transmitter (Glu) that consequently induces diseases (Hartley et al., 1993) by inducing neuronal cell death

(Szatkowski and Attwell, 1994). As Glu is the major neurotransmitter in the brain, a chemical imbalance of this amino acid would produce serious damage in the nervous system. Glu excess kills neurons by prolonged receptor-mediated depolarization (Gasic and Hollman, 1992).

Glutamate receptors in *Arabidopsis*

Genes for putative amino acid sensors have been identified in *Arabidopsis*, a model plant organism. These genes have high sequence similarity to ionotropic glutamate receptors (iGluRs) in animals (Lam et al., 1998a). *Arabidopsis* ionotropic glutamate receptors (iGLRs) have all the signature features of their animal counterparts, including a plasma membrane signaling peptide, two putative ligand-binding domains, and a "three-plus-one" transmembrane region (Lam et al., 1998a; Chiu et al., 1999) (Fig. 1.2). Because of the sequence homology and structural similarities to animal iGluRs, *Arabidopsis* iGLRs genes are predicted to encode ion channels.

Glutamate gating in plants

In animals, upon binding of glutamate to the receptor gating (opening and closing) of the ion channel occurs. In plants, it appears that Glu may also act as a signaling molecule by possibly binding to *Arabidopsis* GLRs. Physiological evidence of Glu-gating in plant ion channels has been reported by Dennison and Spalding (2000). By using transgenic *Arabidopsis* seedlings expressing aequorin, a calcium sensitive luminescent protein (Knight et al., 1991). These authors observed that upon addition of glutamate to root tip cells of the transgenic *Arabidopsis* seedlings there is an increase in

cytosolic Ca^{2+} fluctuation, which is consistent with the influx of Ca^{2+} across the plasma membrane. It was suggested that GLR channels are mediating these Ca^{2+} fluctuations, which is an important mechanism for signal transduction.

Recently glycine, which is required as a co-agonist to activate the mammalian NMDA receptors (Johnson and Ascher, 1987; Kleckner and Dingledine, 1988) has been postulated to play a role in activating At*GLR* (Dubos et al., 2003). Dubos et al. (2003) measured cytosolic Ca^{2+} fluctuations in transgenic *Arabidopsis* seedlings expressing aequorin (Knight et al., 1991). They found that Glu and glycine induce an increase in cytosolic Ca^{2+}, suggesting that glycine and Glu act synergistically to activate plant NMDA receptors. They further suggest by using a docking algorithm and a molecular model of the ligand-binding domain of the GLR receptors that glycine and not Glu is likely the natural ligand for the majority of plant GLRs.

Evidence for the presence of glutamate receptors in plants

To assess the function of putative GLR genes in plants, *Arabidopsis* seedlings were treated with the iGluR inhibitor, 6,7-dinotroquinoxaline-2, 3-(1H, 4H)-dione (DNQX) which is known to block AMPA/Kainate iGluRs in animals. DNQX inhibits two key processes in seedling photomorphogenesis in *Arabidopsis*: light-induced hypocotyl shortening and light-induced greening (Lam et al., 1998a). Dark-grown seedlings were not affected by DNQX, indicating its effect is light specific. Similar morphological results were obtained with S(+)-β-methyl-α, β- diaminopropionic acid (BMAA), a cycad-derived glutamate receptor agonist (Brenner et al., 2000). This observation is particularly interesting since BMAA, an iGluR agonist, causes symptoms similar to

those of DNQX, an iGluR antagonist. These two neurotoxic compounds affect photomorphological aspects of the hypocotyl in the *Arabidopsis* seedlings, suggesting that the plant GLRs may be involved in light signal transduction (Lam et al., 1998a; Brenner et al., 2000). The reason why both an iGluR inhibitor and an agonist give the same morphological effect is unknown. One possibility is that the inhibitor's action and the desensitization of the channel by the agonist lead to similar consequences by binding to the same domain in an enzyme.

Predicted function of GLRs in *Arabidopsis*

Plant GLRs have been predicted to function as Ca^{2+}-permeable channels (Davenport, 2002). Overexpression of *AtGLR*3.2 in *Arabidopsis* seedlings disrupts calcium homeostasis and induces hypersensitivity to K^+ and Na^+ ions (Kim et al., 2001). Kim et al. suggested that overexpression of *AtGLR*3.2 induces uptake of K^+ and Na^+ by being permeable to Ca^{2+} ions. Expression of *AtGLR*3.7 (Cheffings, 2001) and *AtGLR*3.4 (Lacombe et al., 2001a) in *Xenopus* oocytes indicates that plant glutamate receptors are likely mediators of Ca^{2+} ions through the plasma membrane. Recently, the first evidence of the involvement of plant GLRs in Carbon/Nitrogen signaling was provided by Kang and Turano (2003). Using transgenic antisense *AtGLR*1.1 *Arabidopsis* lines, they observed a decrease of C- and N-metabolic enzymes due to the reduction of *AtGLR*1.1 in the *Arabidopsis* seedlings. However, the authors also observed that the *AtGLR*1.1 deficient seedlings exhibit sensitivity to increased levels of Ca^{2+} and react to iGluR agonist (DNQX) and antagonist (BMAA) as well as Glu. This observation prompted them to suggest that *AtGLR*1.1 may additionally function as a receptor mediating Ca^{2+}.

BMAA a glutamate receptor agonist

S(+)-β-methyl-α, β-diaminopropionic acid (BMAA) is known to act as a glutamate receptor agonist in the mammalian nervous system (Weiss et al., 1989, 1991). The specific mode of action of BMAA and its molecular targets are still poorly understood. One hypothesis is that the glutamate receptors in plants mediate BMAA action. Because the effect of BMAA on glutamate receptors has been linked to neurodegenerative disorders in humans (Spencer et al., 1987; Weiss et al., 1991), identifying the function of BMAA, potentially through its action on glutamate receptors in plants is of fundamental importance, as it would potentially lead to the understanding and treating of glutamate receptor related diseases in humans.

Neurotoxic properties of BMAA

BMAA is neurotoxic on glutamate receptors in animals (Weiss et al., 1988, 1989, 1991). Because, BMAA (Fig. 1.3B) lacks the dicarboxylic acid structure present in glutamate (Fig. 1.3A), which is supposed to be critical for the excitatory activity, its neurotoxicity has been question. However, it has been shown that BMAA, a cycad-derived (*Cycas circinalis* L.) toxin, at physiological pH, and in the presence of bicarbonate, activates glutamate receptors, producing toxic levels of intracellular calcium in neuronal cells (Brownson, 1996; Weiss et al., 1988). BMAA is claimed to induce neurodegeneration in the Chamorros, the indigenous population of Guam, by causing selective degeneration of neurons in the cerebral cortex and spinal cord (Weiss et al., 1991). BMAA has been linked in the chamorro people as one possible cause of Amyotrophic Lateral Sclerosis - Parkinsonism Dementia complex (ALS-PD), a

neurodegenerative disorder that has affected the Guam population for more than 50 years. The toxicity of the seed has been recognized in the Chamorro tradition. Before consumption, the crushed cycad seed was regularly water-washed for a number of days. This washing is known to significantly reduce the BMAA concentration in the final product (Duncan et al., 1989, 1990; Wilson et al., 2002; Khabazian et al., 2002).

Several studies (Duncan et al., 1989, 1990; Khabazian et al., 2002; Wilson et al., 2002) question whether the residual amounts of BMAA left in the cycad flour, although minimal, are enough to cause ALS-PD complex. However, recently, the ALS-PD complex disease in Guam has been suggested to be the result of a significant ingestion of cycad toxins by consumption of the Guamanian flying foxes, which are a common feast in the Chamorro culture (Cox and Sacks, 2002; Banack and Cox, 2003). By feeding on cycad seed, flying foxes accumulate toxic levels of cycad neurotoxins.

Vega and Bell (1967), who originally isolated and identified BMAA, found it to be highly neurotoxic to chicks in preliminary experiments. Weiss et al. (1988, 1989), who investigated the toxicity on cultured mouse cortical neurons, also found BMAA to be neurotoxic with bicarbonate required as a toxic cofactor. Other evidence suggests that BMAA is a low-potency toxin (Charlton et al., 1992) and acts as a glutamate receptor agonist only at high dose rates (Seawright et al., 1999).

BMAA activates intracellular Ca^{2+} in animals

It is presumed that in animals Ca^{2+} influx may activate other Ca^{2+} dependent signaling pathways. When Ca^{2+}-dependent signal cascades are disrupted, altering Ca^{2+} homeostasis, neuron cell death occurs (Choi, 1988). Excess of Ca^{2+} influx through

NMDA receptor-channels is a key step in triggering neuronal death induced by brief intense exposure to Glu (Hartley et al., 1993). In order to determine if Ca^{2+} overload is involved in excitotoxicity in animals, Brownson (1996) tested if BMAA induces intracellular Ca^{2+}. The results showed that BMAA not only elevates the level of intracellular calcium to toxic levels killing neurons, but also that Ca^{2+} increase depends directly on the concentration of bicarbonate and extracellular Ca^{2+}. Brownson (1996) suggested that the molecular configuration between BMAA and bicarbonate may be appropriate to activate the receptors and to create the neurotoxicity attributed to BMAA by increasing intracellular Ca^{2+} levels.

Theme of the thesis

The experiments described in this dissertation are aimed at defining the role of the putative glutamate receptors in plants by using BMAA, an animal glutamate receptor agonist. An introduction to the topic is given in Chapter 1.

Chapter 2 presents material upon which a paper published in the journal Plant Physiology (Brenner et al., 2000) was based. I am the second author of this publication, which displays the photomorphogenic effects of BMAA on *Arabidopsis* and defines the *bim* screen whose importance lies in the introduction of the *bim* mutants and their classification into three classes. My work consisted in (1) preparing all the materials for and conducting the screen that generated ten identified *bim* mutants; (2) generating and analyzing the results which includes the pictures depicting the *bim* mutants, and the data and graphs illustrating the quantification of the *bim* hypocotyls' responses.

Chapter 3 consists of a manuscript that is prepared for submission for publication (Barboza et al., 2004). This paper is important as it identifies three of the ten previously published *bim* mutants, describes the cloning of a Class II *bim* mutant and its characterization, and describes a model postulating the interaction between BMAA and two *BIM* loci. It also provides evidence that allows one to hypothesize regarding the function of BMAA in cycads. This chapter has an appendix with additional information that was not included in the manuscript.

Chapter 4 describes an attempt to determine possible ways by which BMAA may interact with *Arabidopsis iGLRs*. I include a model suggesting how BMAA may mediate Na^+ and K^+ ions in *Arabidopsis* seedlings.

Figure 1.1. Transmission at a Chemical Synapse. The binding of a neurotransmitter (Glu) at the ligand-binding domain makes the channel permeable to ions. The flow of these ions into and out of the cell depolarizes the cell membrane, triggering a signal.

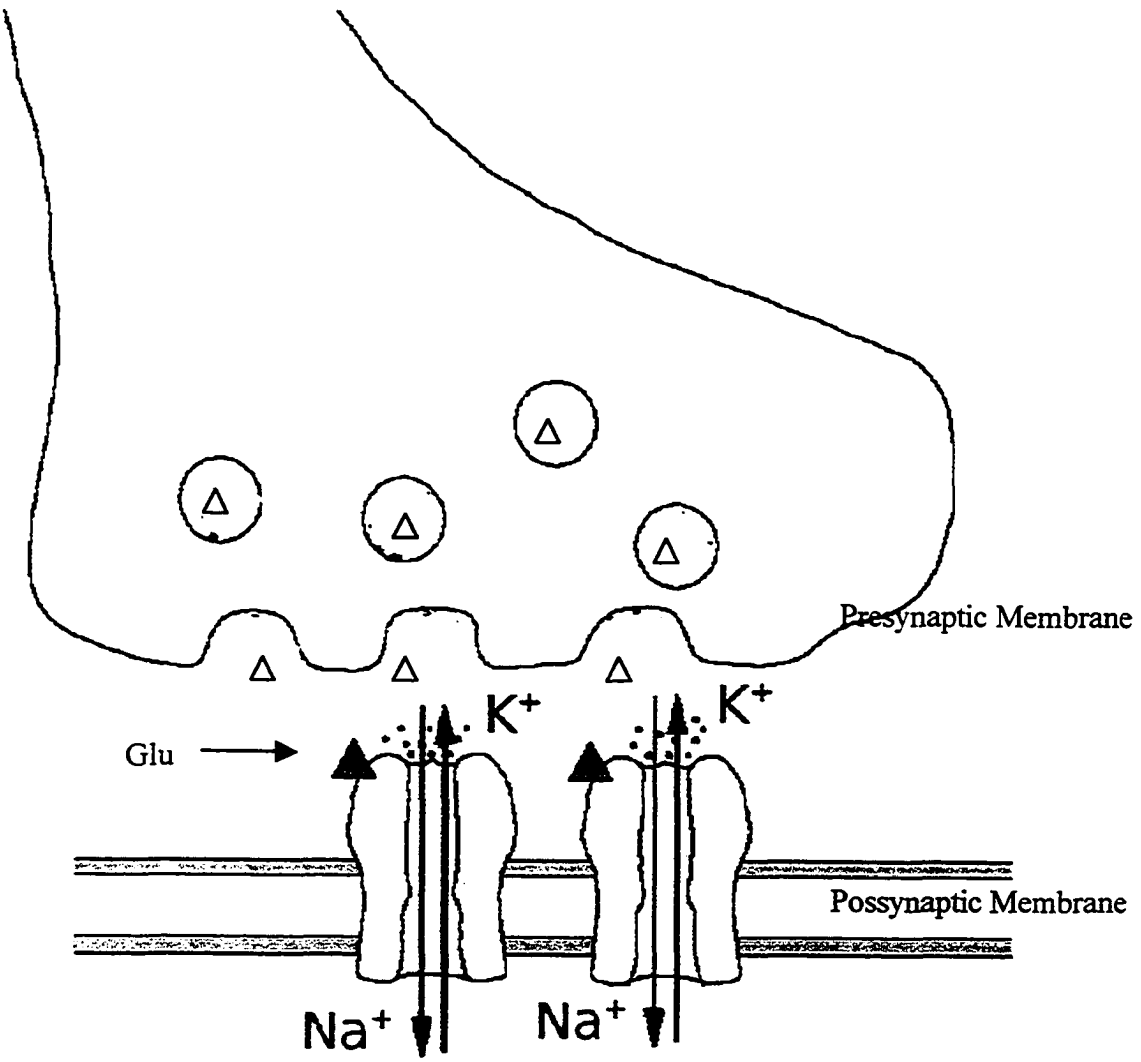

Figure 1.2. Schematic of an *Arabidopsis* Glutamate Receptor Subunit. The subunit contains three transmembrane domains (M1, M3, and M4), an internal re-entrant membrane loop (M2), a conserved ligand-binding domain (S1, S2), an extracellular N-terminal and intracellular C-terminal.

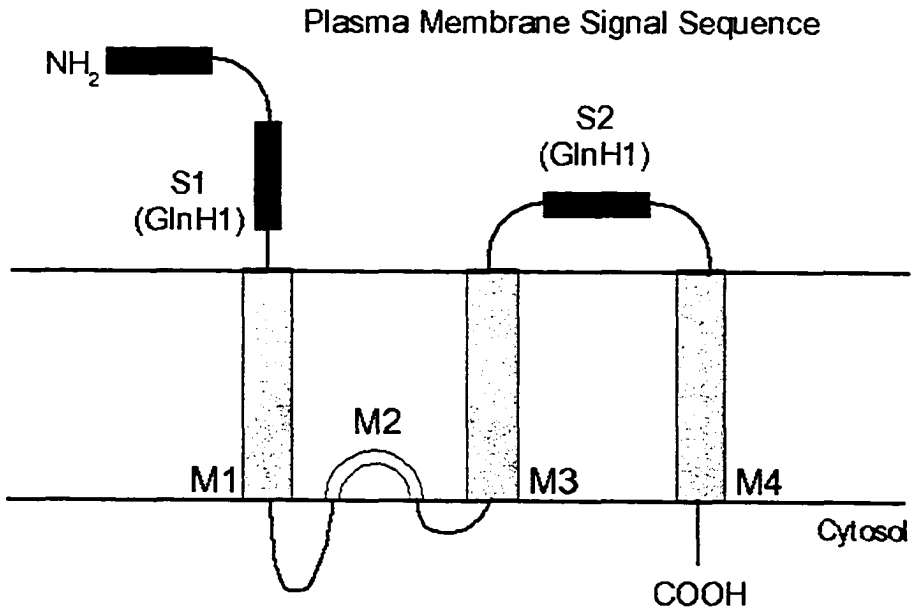

Figure 1.3. Chemical Structure of Glutamate and BMAA. (A) Structure of Glutamic acid. **(B)** Structure of BMAA. BMAA lacks the dicarboxylic acid structure thought to be critical for the excitatory activity.

A

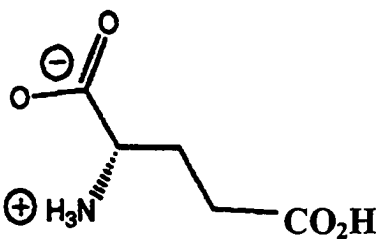

B

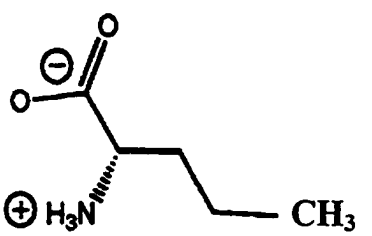

CHAPTER 2

Arabidopsis Mutants Resistant to S(+)-β-Methyl-α, β-Diaminopropionic Acid, a Cycad-Derived Glutamate Receptor Agonist

ABSTRACT

In the mammalian nervous system, glutamate receptors (GluR) are ligand-gated ion channels involved in rapid synaptic transmissions. Genes encoding for homologous ionotropic glutamate receptor (GLR) were identified in *Arabidopsis*. To understand the function of the putative ionotropic glutamate receptor genes in plants, *Arabidopsis* seedlings were treated with a mammalian glutamate receptor agonist, S(+)-β-methyl-α, β-diaminopropionic Acid, (BMAA). BMAA affects photomorphogenesis of *Arabidopsis* seedlings by inducing a two-to-three fold hypocotyl elongation and inhibiting cotyledon opening. This effect is specific to light, because BMAA has no effect on elongation of etiolated seedlings. To identify the molecular targets of BMAA, a forward genetic screen was used to isolate *Arabidopsis* mutants insensitive to the effects of BMAA on photomorphogenesis. These are called "BMAA insensitive morphology" (*bim*) mutants. The *bim* mutants, when grown in the presence of 50μM BMAA, have a phenotype similar to that of untreated plants: short hypocotyl and open cotyledons. In the light in the absence of BMAA, the *bim* mutants are undistinguishable from the wild type as young seedlings. However, when grown in the dark in the absence and presence of BMAA, the *bim* mutants are subgrouped into three phenotypic classes: Class I *bim* mutants have an etiolated phenotype similar to wild-type plants, Class II *bim* mutants have short hypocotyls and closed cotyledons and Class III *bim* mutants have short hypocotyls and open cotyledons similar to the constitutively photomorphogenic mutants, *cop/det/fus*. Fine-mapping of the *bim* mutants will help elucidate the different biochemical pathways affected by BMAA in the mutants and whether any of these pathways is linked to GLRs signaling in plants.

INTRODUCTION

Ionotropic glutamate receptors (iGluR) are the predominant neuroreceptors in the mammalian central nervous system and have major roles in fast synaptic transmissions (Dingledine et al., 1999). Glutamate (Glu) is the major excitatory neurotransmitter in the vertebrate brain and activates iGluR at the post-synaptic membrane. iGluRs are pharmacologically classified in three separate classes based on selective activation with different glutamate analogues (MacDermott, 1987; Dingledine et al., 1999): N-methyl-D-Aspartate (NMDA), alpha-amino-3-hydroxy-5-methylisoxazole-4-propionic acid (AMPA), and Kainic acid (Kainate). The latter two categories are collectively referred as 'non-NMDA receptors'.

In plants, glutamate signaling has been shown to affect expression of genes involved with amino acid metabolism (Lam et al., 1998b; Oliveira and Coruzzi, 1999). The mechanisms underlying this signaling are not known at the genetic level, but the possibility that the recently identified homologues of glutamate receptors in *Arabidopsis* (GLRs) are involved in this mediation has been raised (Dennison and Spalding, 2000). The *Arabidopsis* genes share with the iGluR the three transmembrane domains, the re-entrant membrane loop, and the two conserved ligand-binding domains (Lam et al., 1998a; Chiu et al., 1999).

To understand the function of the putative Glu receptors in plants, *Arabidopsis* seedlings were treated with the iGluR inhibitor, DNQX [6,7 Dinotropuinoxaline 2,3 (1H, 4H) dione], known to block nonNMDA iGluRs in animals. DNQX inhibited photomorphogenesis in *Arabidopsis* by inducing hypocotyl elongation and reducing

chlorophyll levels. Dark-grown seedlings were not affected by DNQX; therefore, it is postulated that the putative function of iGLR is involved in light signaling transduction (Lam *et al.*, 1998a). To further understand the molecular function of GLR signaling in plants, an animal iGluR agonist, S(+)-β-methyl-α, β-diaminopropionic Acid (BMAA) was tested on *Arabidopsis* seedlings (Brenner et al., 2000). BMAA is a compound synthesized in cycads, a highly toxic group of plants. BMAA was first identified as being the cause of Amyotrophic Lateral Sclerosis (ALS) and Parkinsonism Dementia complex (PDC), neurodegenerative disorders affecting the Chamorro population in Guam island (Spencer et al., 1987). Because BMAA is suggested to block GluR function in humans, *Arabidopsis* seedlings were submitted to BMAA and evaluated for morphological changes. Light-grown seedlings indicate that the presence of BMAA in the growth medium affects photomorphogenesis by inducing hypocotyl length and inhibiting cotyledon opening and root growth (Brenner et al., 2000). In an attempt to identify *Arabidopsis* glutamate receptor mutant, I used BMAA to screen for mutants insensitive to BMAA. In this study the isolation and preliminary characterization of ten bim mutants is described.

RESULTS

BMAA, a glutamate receptor agonist, affects photomorphogenesis in *Arabidopsis* seedlings

To understand the function of GLR genes in plants, it was determined that iGluR agonist BMAA causes an observable phenotypic effect on plant growth when supplied

to *Arabidopsis* seedlings. Light-grown *Arabidopsis* seedlings were germinated and cultivated in the presence or absence of BMAA. BMAA-treated seedlings were evaluated for phenotypic alterations in treated plants compared with untreated control plants. At 8 days post-germination, the hypocotyls of seedlings grown in the light on 50μM BMAA, displayed elongated hypocotyls (Fig. 2.1 A), compared with control untreated plants (Fig. 2.1B). A dose-dependent response was observed at increasing concentrations of BMAA. The effect of BMAA on hypocotyl elongation was quantified: In light-grown plants, a concentration of 30μM BMAA caused an increase in length of approximately 40% and 50μM BMAA caused approximately a 100% increase in hypocotyl length when compared with untreated plants. The effect on hypocotyl elongation is weaker at 100μM BMAA, and at higher concentrations (200μM) BMAA becomes inhibitory to seedling growth (data not shown). BMAA was also inhibitory to root growth and cotyledon opening (Fig. 2.1A). In the light, the arc of cotyledon opening is reduced to 50° in BMAA-treated plants compared with 110° in control plants (Fig. 2.1A).

Isolation of *Arabidopsis* mutants insensitive to BMAA.

To determine the molecular targets of BMAA, a forward genetic screen was used to isolate *Arabidopsis* mutants resistant to the photomorphogenic effects of BMAA. Mutagenized (M2) *Arabidopsis* seeds were plated and grown in the light on Murashige and Skoog media containing 50μM BMAA. A concentration of 50μM BMAA induces a two- to three- fold hypocotyl elongation and closed cotyledons in wild-type seedlings. M2 plants that exhibited short hypocotyls and open cotyledons when grown on BMAA

were identified as "BMAA insensitive morphology" (*bim*) mutants (Fig. 2.2A). A total of 18,000 ethyl methane sulfonate (EMS) mutagenized seed was grown in the light on 50μM BMAA. In this screen 180 M2 putative *bim* mutants were isolated. The M2 putative *bim* mutants were grown in soil and allowed to self-pollinate. M3 progeny from these plants was tested for genetic inheritance of resistance to the effects of BMAA (Fig. 2.2B). Only ten *bim* mutants inherited the resistance to BMAA (*bim* 18, 26, 40, 50, 77, 131, 136, 167, and 175). Figure 2.2 shows a representative *bim* mutant seedling, *bim* 26, identified in the M2 screen (Fig. 2.2A) and the M3 progeny from this mutant showing the inherited resistance to the BMAA-induce hypocotyl elongation (Fig. 2.2B). All of the *bim* mutations are recessive when backcrossed to wild type.

When treated with 50μM BMAA and grown in the light, wild-type plants have elongated hypocotyls (Fig. 2.3A). In contrast, *bim* mutants have visibly shorter hypocotyls when grown under the same conditions (Fig. 2.3A). When grown in the light without BMAA, *bim* mutants are indistinguishable from wild type as young seedlings (Fig. 2.3B). Figure 2.3 shows two representative *bim* mutants that inherited the resistance to BMAA, *bim*131 and *bim*26. Clearly visible are the shorter hypocotyl of the seedlings, which were grown in 50μM BMAA. Additionally one observes that BMAA treatment impairs root growth in wild-type plants and in the majority of *bim* mutants (Fig. 2.3 A).

The effect of BMAA on hypocotyl length of light-grown plants was quantified for all *bim* mutants, for a *cop* allele, and for wild-type plants (Fig. 2.4A) and was compared with untreated plants (Fig. 2.4B). When grown in the light plus 50μM BMAA, wild type has a two- to three-fold increase in hypocotyl length, compared with

the *bim* mutants, and the *cop* allele (Fig. 2.4A). In contrast, when grown in the light minus BMAA, the majority of *bim* mutants are indistinguishable from the wild type with regard to hypocotyl length, while the *cop* allele shows no difference between the two treatments at the early seedling stage (Fig. 2.4A). Only *bim*131 has a significantly shorter hypocotyl than wild type, when grown in the absence of BMAA (Fig 2.4B).

bim mutants are subgrouped into three separate classes

Because BMAA does not induce morphological changes in etiolated hypocotyls of wild-type seedlings, the *bim* mutants were analyzed in the dark in the absence and presence of BMAA. The *bim* mutants were grouped into three classes based on their morphology when grown in the dark (Fig. 2.5). Class I *bim* mutants (*bim*131, 175) have a normal etiolated morphology, elongated hypocotyls, and closed cotyledons (Fig. 2.5A). Class-II bim mutants (*bim*18, 40, 77, 136, 59, 167) have short hypocotyls but their cotyledons remain closed (Fig. 2.5B). Class-III *bim* mutants (*bim*26 and *bim*50) are constitutively photomorphogenic, have short hypocotyls and display open cotyledons (Figs. 2.5C), similar to the *cop/det/fus* mutants. A representative *bim* mutant, *bim*131 from class I and *bim*26 from Class III, are illustrated in figure 2.6. Each has visibly shorter hypocotyls when grown in the light on 50μM BMAA (Fig. 2.6A). When grown in the dark either in the absence or presence of BMAA, *bim*131 has an etiolated phenotype and *bim*26 is constitutively photomorphogenic (Fig. 2.6B). The effects of BMAA on a representative *cop* mutant (*cop 1-6*) are depicted in Figures 2.4 and 2.7. BMAA has no effect on hypocotyl elongation of the *cop1-6* mutation in the light (Fig.

2.4) or in the dark (Fig. 2.7). In contrast, BMAA causes a slight decrease in the hypocotyl length of *bim* mutants in the light and in the dark.

DISCUSSION

This study provides evidence that BMAA, a plant-derived agonist that blocks Glu receptor function in animals, alters early morphogenesis of light-grown *Arabidopsis* seedlings. BMAA induces hypocotyl elongation and inhibits cotyledon opening specifically in light-grown plants. These effects of BMAA on *Arabidopsis* seedlings are reminiscent of the long hypocotyl of "hy" mutants defective in sensing light and/or transmitting light signals in *Arabidopsis* (von Arnim and Deng, 1996). Our lab reported previously that DNQX, an antagonist of AMPA/Kainate receptors in animals, also causes hypocotyl elongation when added to the growth media of *Arabidopsis* seedlings (Lam et al., 1998a). The fact that DNQX, a GluR antagonist, and BMAA, a GluR agonist, each induce hypocotyl elongation in light-grown seedlings provides support for the hypothesis that endogenous plant GLR genes may be involved in photomorphogenic development in *Arabidopsis*. DNQX (an iGluR antagonist) could potentially antagonize *Arabidopsis* GLRs, which may be involved in light-mediated inhibition of hypocotyl growth. BMAA as an agonist could possibly affect GLR signaling by desensitizing the channels and driving them to a nonconductive state or persistently activate them similar to Glu, the native GluR agonist (Nakanishi, 1992; Wisden and Seeburg, 1993). The observation that BMAA effects are abrogated in a dose-dependent manner by Glu (Brenner et al., 2000) suggest that in *Arabidopsis* increasing levels of Glu would

displace or prevent the binding of BMAA on-binding sites restoring normal photomorphogenic conditions. These results support the hypothesis that BMAA may act by blocking AtGLR signaling in *Arabidopsis*. In animals, iGluRs after activation become inactive by either a weakening of agonist affinity or desensitization when channels enter a long-lived nonconducting state (Sun et al., 2002). In animals Glu desensitization is necessary for proper iGluR gating. The fact that Glu, the native GluR agonist, in addition to its normal function as an excitatory neurotransmitter in the brain, can also kill neurons by persistently activating the channels (Nakanishi, 1992; Wisden and Seeburg, 1993), supports the hypothesis that BMAA impairs iGluR function by a similar mechanism. Membrane depolarization activated by anion channels is believed to be a signal-transduction event leading to inhibition of hypocotyl elongation (Cho and Spalding, 1996; Lewis et al., 1997). In this scenario, I hypothesize that BMAA induces hypocotyl elongation by blocking AtGLR signaling that leads to photomorphogenesis.

To test this hypothesis and to determine the molecular targets of BMAA, a genetic screen using BMAA was used to isolate *Arabidopsis* mutants insensitive to the effects of BMAA. The aim was to uncovered mutants with GLR lesions and to elucidate the molecular targets of BMAA on *Arabidopsis*. Ten BMAA insensitive morphology (*bim*) mutants were isolated. These *bim* mutants were separated into three classes based on their dark-grown morphology. Class I includes *bim* mutants (*bim*131 and *bim*175) with an etiolated hypocotyl similar to wild type. Members in Class I resemble those mutants defective in ethylene receptors (Chang and Meyerowitz, 1995). Dominant, gain of function ethylene receptor mutants (etr 1-1) are insensitive to the photomorphogenic effects of BMAA (data not shown) and have an etiolated phenotype in the dark. Class II

bim mutants (*bim*18, 40, 77, 136, 167) have short hypocotyls and closed cotyledons. These mutants have a dark-grown phenotype similar to *procuste* (Desnos et al, 1996) a cell wall mutant (Fagard et al., 2000). Class III *bim* mutants (*bim*26 and *bim*50) have short hypocotyl and open cotyledons reminiscent of the constitutively photomorphogenic *cop/det/fus* mutants (Deng et al., 1991; Chory et al., 1989, Miséra et al., 1994). The effect of BMAA was tested on a constitutively photomorphogenic mutant *cop* 1-6 (Fig. 2.5 and 2.8). BMAA does not affect elongation of the *cop*1-6 hypocotyls in the light or in the dark. Conversely BMAA decreases hypocotyl length of *bim*26 (Fig. 2.5 and 2.8) in light and dark conditions. Genetic complementation has confirmed that *bim*26 is an allele of *cop*11 (G.M. Coruzzi Laboratory, unpublished data). Why BMAA affects photomorphogenesis of *bim*26 but not of *cop*1-6 is not known. One could speculate that the wild-type products from these two mutations interact differently with BMAA.

Plant growth and development requires the integration of signals from diverse environmental factors. Light exposure and plant hormones play an important role in such complex interactions. Some phytohormones such as auxin (Evans, 1985) and gibberellin (Jacobsen and Olszewski, 1993) promote elongation of the hypocotyl, while ethylene (Abeles et al., 1992) and cytokinins (Chory et al., 1991) inhibits the hypocotyl elongation. The fact that *etr*1-1 and *aux*1-3 with a normal etiolated morphology are insensitive to induction of hypocotyl elongation by BMAA (data not shown) suggests that BMAA effects on hypocotyl length in light-grown plants may involve the interaction of one or more of these phytohormones.

It appears that addition of BMAA to *Arabidopsis* affects normal photomorphogenesis. Therefore, the presence of BMAA in cycads is a puzzling question. Field studies have revealed that plant species, by using chemical means, compete either for resources or survival (Whittaker and Feeny, 1971) and members of the Cycadales have survived predation and climatic changes for at least 250 million years. Thus it seems reasonable to assume that the presence of BMAA in cycads is a mechanism developed for survival and defense. BMAA has been suggested to act as a toxin against general predation by animals and phytophager insects and as a factor in regulating cone pollination by insects (Vovides et al., 1993). Whether BMAA additionally acts as a signaling compound affecting the function of AtGLR in cycads or mediating other light signaling pathways are open questions that remain to be answered. Fine-mapping *Arabidopsis bim* mutants may help address these questions.

MATERIALS AND METHODS

Plant growth conditions

After surface-sterilization, *Arabidopsis* ethyl methane-sulfonate mutagenized seed (Lehle Seeds, Round Rock, TX) was platted on Murashige and Skoog (Sigma) media supplemented with 1% sucrose, and 8% agar. The pH (5.7) was adjusted before the addition of agar. 50μM BMAA (Sigma G-1501) was added after the medium was sterilized and cooled to 50°C. Seed was pretreated for 3 days @ 4°C, before grown vertically in square plates (100 x 15mm) for 7 days. Selected M2 plants that showed resistance to BMAA were grown in metromix 200 (Grace, Sierra) in 16 hours light 8

hours dark cycle at 22°C in a plant growth chamber. From 180 M2 putative *bim* mutants selected only 10 inherited the resistance to BMAA.

Root and hypocotyl measurements

The Roots and hypocotyls of 20 seedlings for each treatment were measured with a ruler under a stereoscope.

Fig. 2. 1. Effects of BMAA on *Arabidopsis* seedlings. BMAA causes hypocotyl elongation and inhibits cotyledon opening in light grown seedlings. *Arabidopsis* seedlings were grown in the light for 7 days.

(A) In the presence of 50μM BMAA

(B) In the absence of BMAA

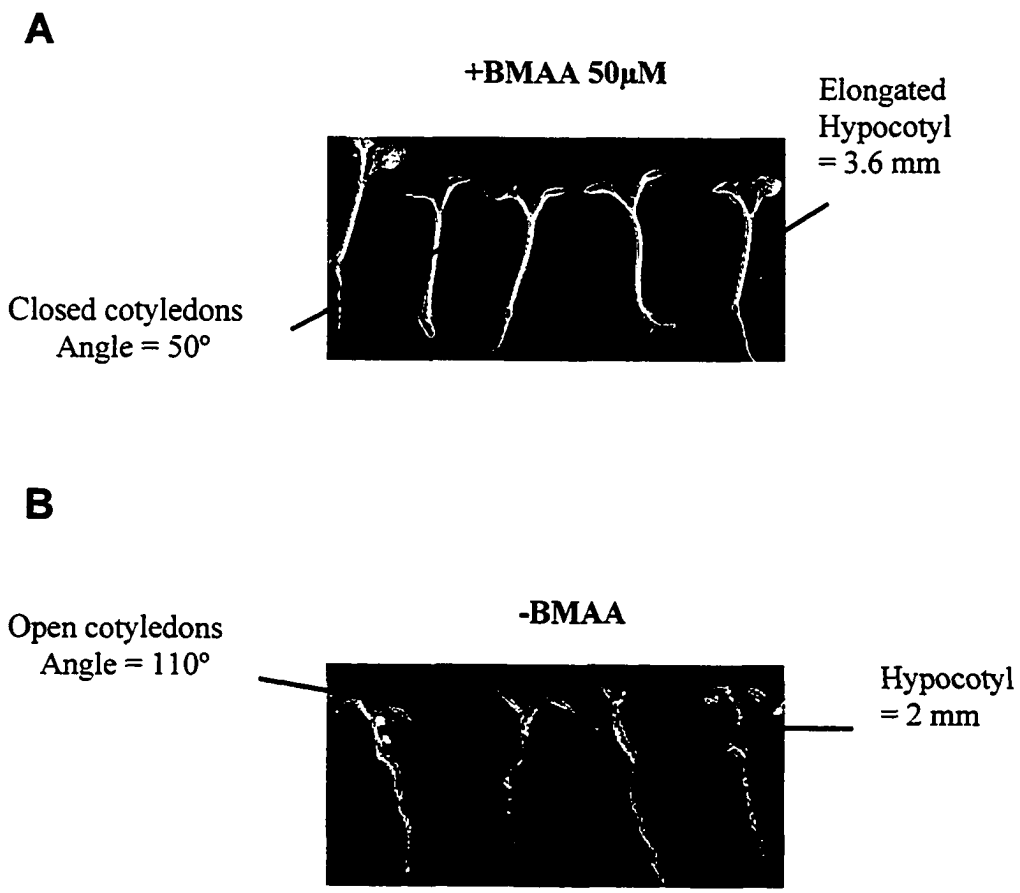

Figure 2.2. Genetic screen to isolate BMAA insensitive morphology (*bim*) mutants.

Light-grown seedlings grown in 50μM BMAA.

(A) A representative M2 *bim* mutant, *bim* 26.

(B) M3 progeny of *bim* 26 that inherited the resistance to BMAA is compared to wild-type seedlings (left).

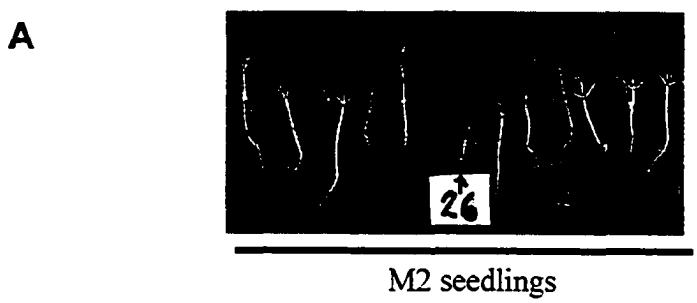

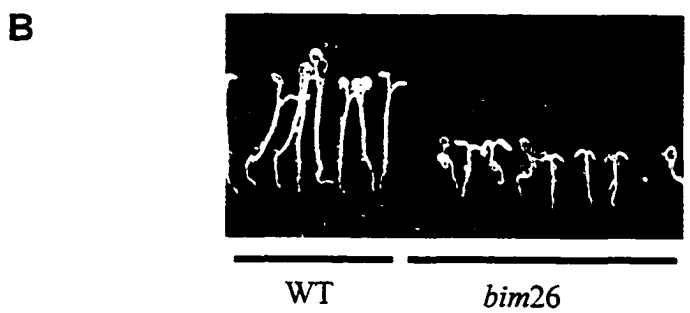

Figure 2.3. *bim* mutants are insensitive to BMAA. Two representative M3 *bim* mutants (*bim* 26 and *bim* 131) were grown for 5 days in the light. In 50μM BMAA, both mutants (right) have short hypocotyls when compared to the control wild type (left). In the absence of BMAA both mutants are indistinguishable from wild-type seedlings.

(A) In medium containing 50μM BMAA.

(B) In the absence of BMAA.

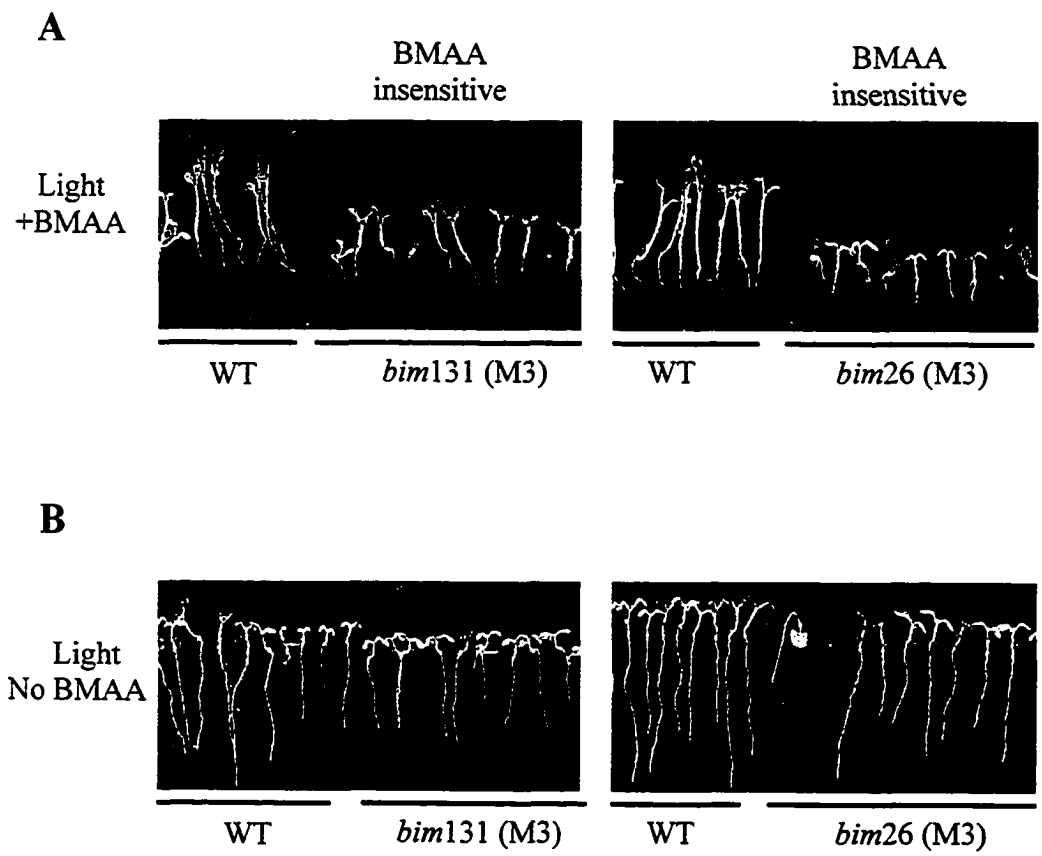

Figure 2.4. Quantification of the hypocotyl length of *bim* mutants grown in the light in the presence and absence of BMAA. The hypocotyl length of the 10 *bim* mutants is compared to those of the *cop1-6* mutant and to wild-type seedlings.

(A) In the presence of 50μM BMAA

(B) In the absence of BMAA

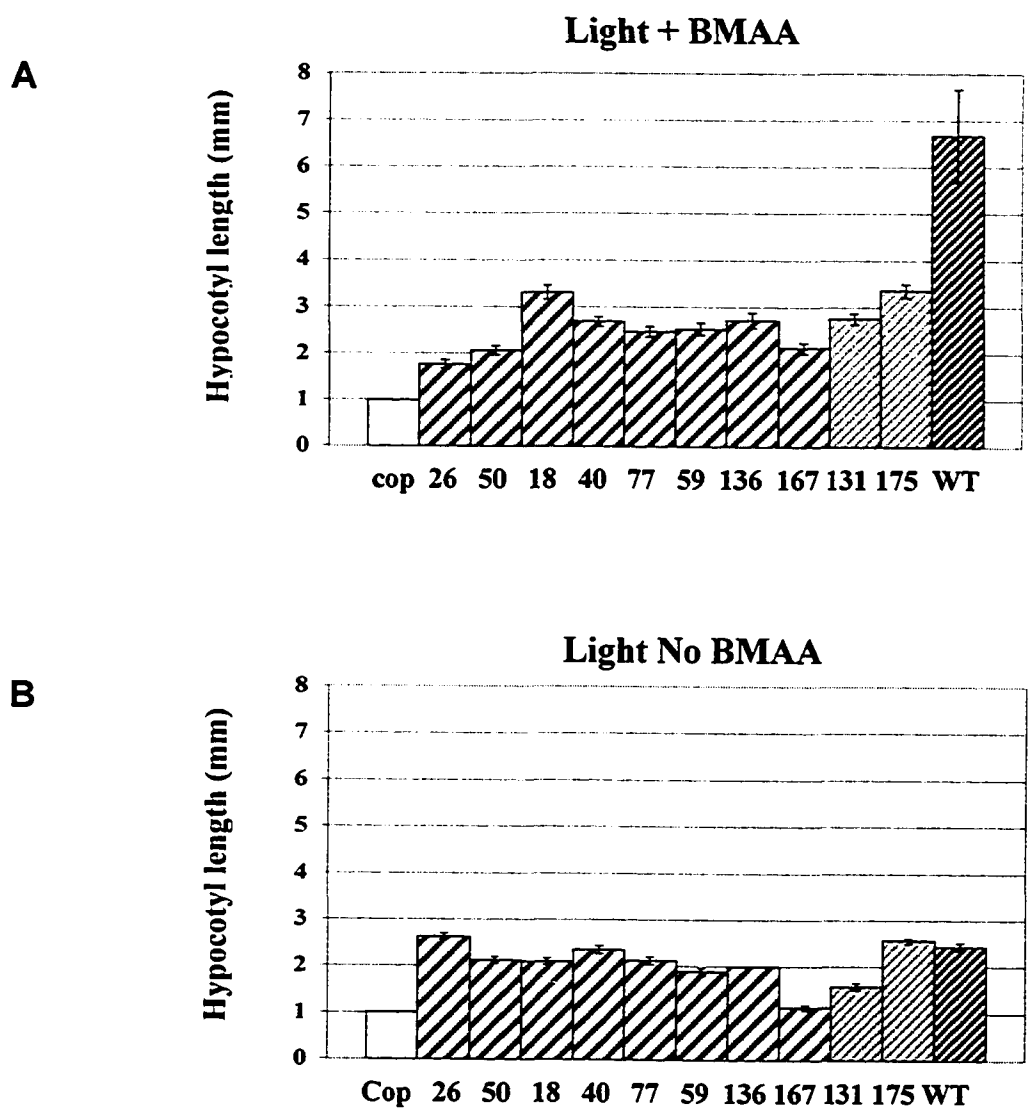

Figure 2. 5 *bim* mutants fall into three separate classes based on their dark-grown morphology. Seedlings were grown in the dark in the absence of BMAA during 5 days. A representative *bim* mutant from each class is compared to wild-type seedlings (right).

(A) Class I *bim* mutants have an etiolated phenotype similar to wild type.

(B) Class II *bim* mutants have short hypocotyl and closed cotyledons.

(C) Class III *bim* mutants are constitutively photomorphogenic.

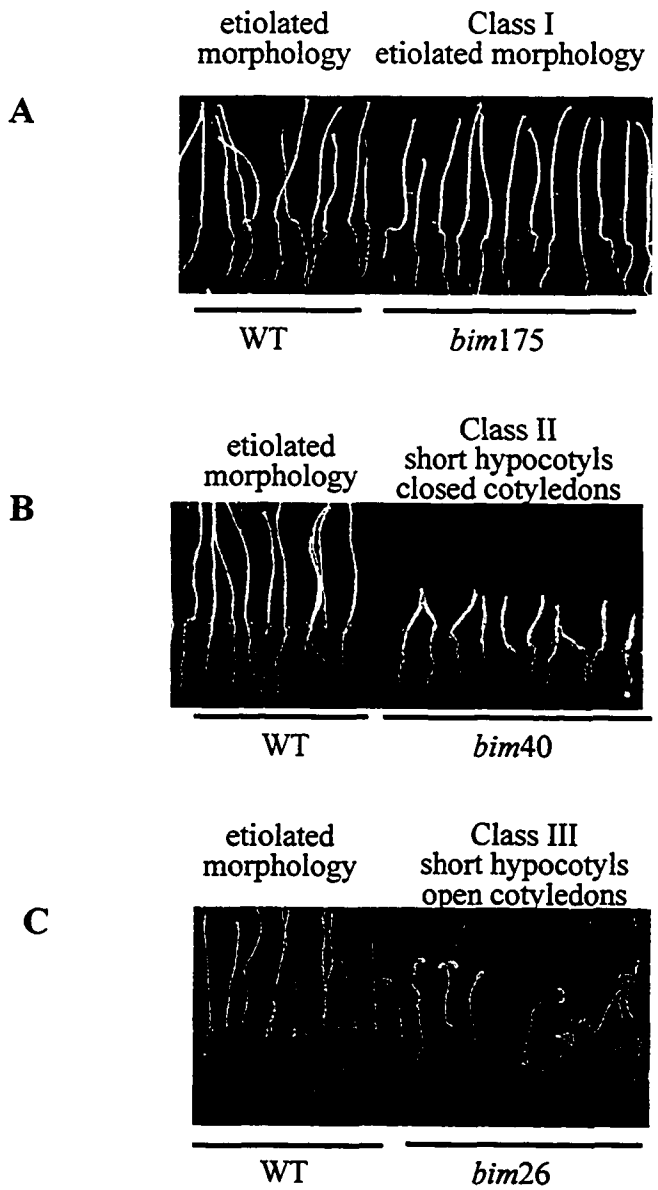

Figure 2.6. Two representative *bim* mutants resistant to iGluR agonist, BMAA.

(A) In the light, *bim*131 and *bim*26 are insensitive to BMAA when compared to wild type.

(B) In the dark, *bim*131 from class I has an etiolated phenotype, while *bim*26 from class III is constitutively photomorphogenic.

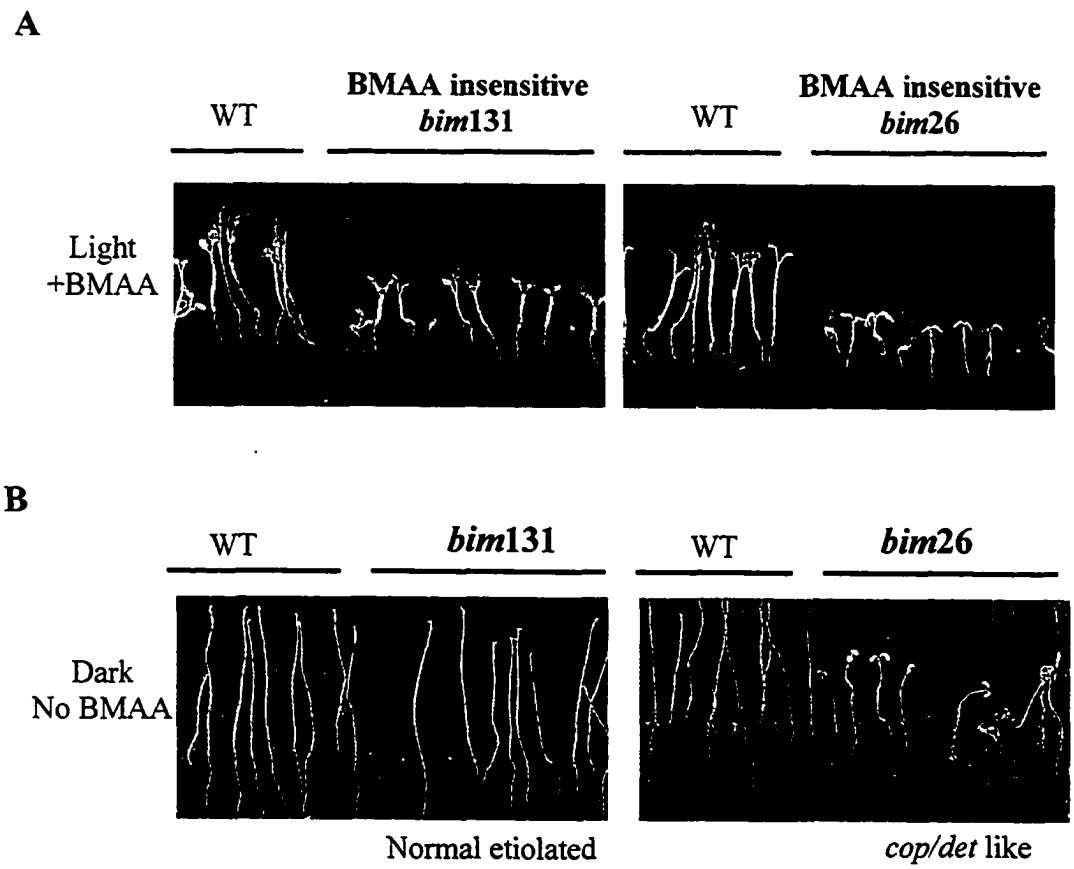

Figure 2.7. Quantification of the hypocotyl length of *bim* mutants grown in the dark in the presence and absence of BMAA. The hypocotyl length of the 10 *bim* mutants is compared to those of the *cop1-6* mutant and to wild-type seedlings The hypocotyl length of the *bim* mutants is represented within classes.

(A) In the presence of 50μM BMAA

(B) In the absence of BMAA

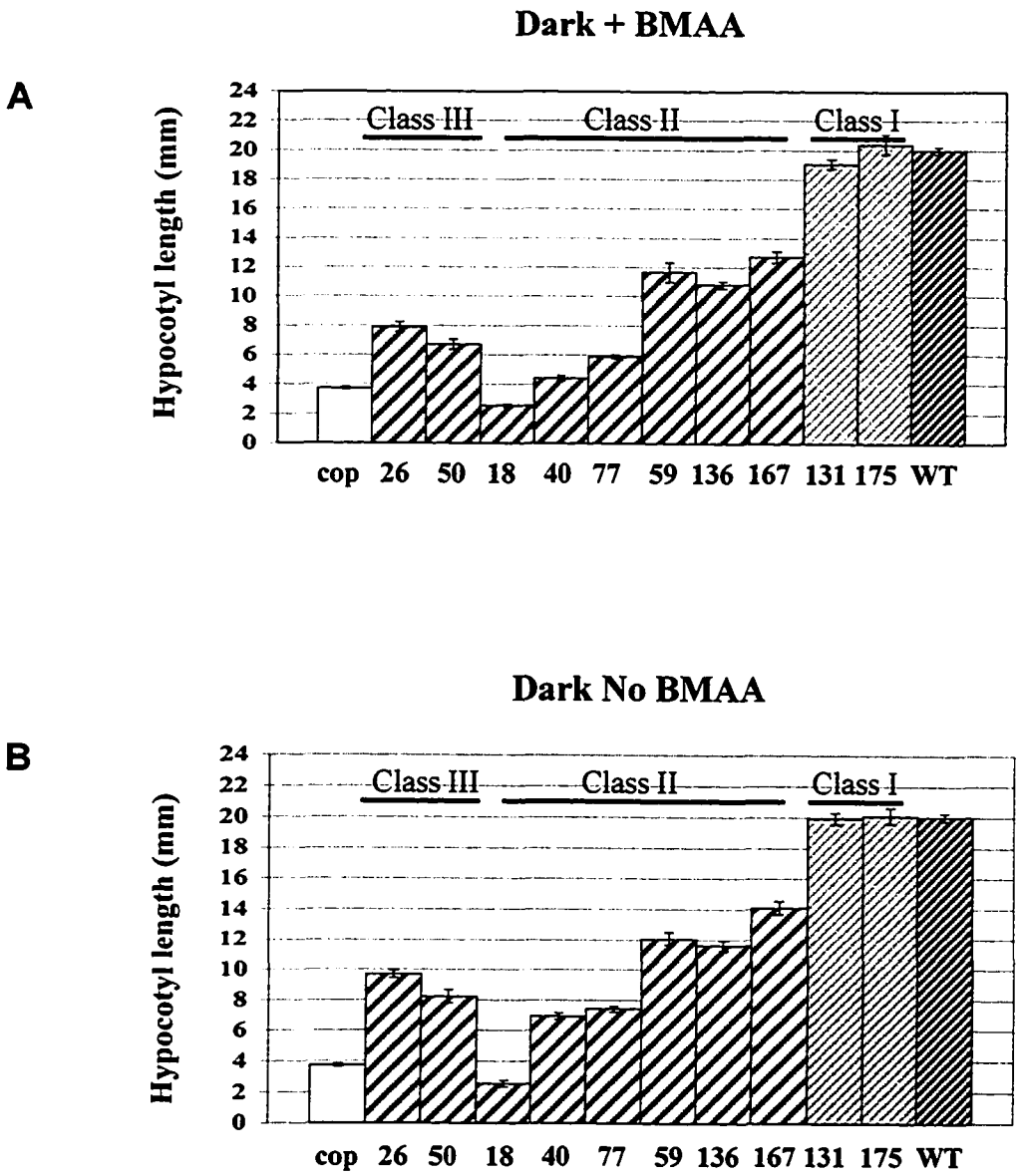

Chapter 3

Genetic Complementation of the *bim* Mutants and Positional Cloning of *bim*4, a Class II BMAA-Insensitive Mutant

ABSTRACT

In the mammalian nervous system, glutamate receptors are the predominant ligand-gated receptor channels. Plants possess genes (*AtGLR*) with high sequence similarity to those animal ionotropic glutamate receptors (iGluR). Using the animal iGluR agonist, S(+)-β-methyl-α-, β-diaminopropionic acid (BMAA), in a genetic screen designed to study physiological and biochemical functions of *AtGLRs* in *Arabidopsis*, BMAA-insensitive morphology (*bim*) mutants were isolated. BMAA in wild-type *Arabidopsis* seedlings induces hypocotyl elongation, and inhibits both cotyledon opening and root growth. In contrast, *bim* mutants have short hypocotyls and open cotyledons on BMAA. Two *BIM* loci were characterized using genetic mapping, complementation, and sequence analysis. Genetic complementation analysis revealed that *bim*3 is an allele of *procuste* (*prc*), a cellulose synthase mutant, and sequence analysis confirmed that *bim*4 is allelic to a glycosyl hydrolase (chitinase) mutant, named *AtCTL1* (*ELP1*). It was observed that both *bim*3 and 4 mutations confer cell wall rupture in the cortical tissue of the hypocotyl. I propose that *bim3* and *bim4* mutants are resistant to BMAA due to their inability to elongate their cell wall. I also propose a model depicting the impact of BMAA on the regulation of *PRC1* and *CTL1* expression.

INTRODUCTION

In plants, glutamate (Glu) may function as a signaling molecule, altering transcription of key enzymes involved in amino acid metabolism (Lam et al, 1998b; Oliveira and Coruzzi, 1999). How these signals are perceived is not known at the genetic level. It has previously been suggested that putative ionotropic glutamate receptor-like genes (*AtGLR*) in *Arabidopsis* may be involved in amino acid signaling (Lam et al. 1998a; Chiu et al., 1999). The *Arabidopsis* ionotropic glutamate receptors (GLRs) preserve all the important domains predicted to encode ion channels, including the two ligand-binding domains, and the four transmembrane segments (Lam et al., 1998a; Chiu et al., 1999). Although it is unclear whether *AtGLRs* are involved in amino acid signaling, they have been predicted to be mediators of Ca^{2+} ions. Overexpression of *AtGLR*3.2 in *Arabidopsis* seedlings disrupted calcium homeostasis (Kim et al., 2001) and *AtGLR*1.1 deficient *Arabidopsis* lines were found to have reduction of C- and N-metabolic enzymes as well as hypersensitivity to Ca^{2+} (Kang and Turano, 2003).

Direct physiological evidence of glutamate signaling has been reported (Dennison and Spalding, 2000) in that glutamate induces changes in the cytosolic Ca^{2+} concentration and mediates membrane depolarization in *Arabidopsis* root cells. Recently glycine, co-agonist of the mammalian NMDA receptor (Johnson and Ascher, 1987; Kleckner and Dingledine, 1988), was similarly found to trigger increases of cytosolic Ca^{2+} in *Arabidopsis* seedlings (Dubos et al., 2003).

Previous studies suggested that Glu ligand-gated ion channels could be a key component of signal transduction involved in regulating developmental aspects of plants. Assays with two compounds known to interfere with AMPA and Kainate

receptor function (Lobner and Lipton, 1993; Weiss et al., 1989, 1991), namely the iGluR antagonist 6,7-Dinotroquinoxaline 2, 3 (1H, 4H)-dione (DNQX; Lam et al., 1998a) and the agonist S(+)-β-methyl-α-, β-diaminopropionic acid (BMAA; Brenner et al., 2000), suggest that plant *GLRs* may be involved in light signal transduction. *Arabidopsis* seedlings treated with DNQX and BMAA display a phenotype reminiscent of "hy" mutants (von Arnim and Deng, 1996), which are impaired in light signal perception as exhibited by elongated hypocotyls when grown in the light (Lam et al., 1998a; Brenner et al., 2000).

In an attempt to isolate mutants in *AtGLR* signaling pathways, I have previously reported a screen to uncover *bim* mutants (Brenner et al., 2000). Since BMAA is a known animal iGluR agonist, I predict that it might also activate plant GLRs. Therefore *bim* mutants might be imparied in AtGLR signaling pathways. When grown in the light on 50μM BMAA, *Arabidopsis* seedlings displayed elongated hypocotyls, inhibition of both root growth and cotyledon opening. However, BMAA insensitive morphology (*bim*) mutants, grown in the presence of 50μM BMAA, displayed a phenotype similar to that of untreated plants; that is, short hypocotyls and open cotyledons. Ten *bim* mutants were isolated (*bim18, 26, 40, 50, 59, 77, 131, 136, 167*, and *175*) and grouped into three classes based on their morphology when grown in the dark either in the presence and absence of BMAA. Class I *bim* mutants (*bim*131 and 175) have an etiolated morphology similar to that of wild-type plants. Class II *bim* mutants (*bim*18, 40, 59, 77, 136 and 167) each have short hypocotyls and their cotyledons remain closed. Class III *bim* mutants (*bim*26 and 50) are constitutively photomorphogenic, i.e they have short hypocotyls and display open cotyledons in the dark. Because it appears that the mutations conferring BMAA-insensitivity in Class II and III mutants affect aspects

of skotomorphogenesis, I postulate that these mutants disrupt morphogenic targets downstream of photoperception. I am interested in what constitutes Class II and Class III mutants; here I focus on three *bim* mutants from Class II and report on the positional cloning of two of these *bim* mutants. Additionally I define complementation groups among the *bim* mutants.

RESULTS

Complementation grouping of *bim* mutants

To determine the number of *bim* loci isolated from the screen described in Brenner et al. (2000), genetic complementation tests were performed between *bim* mutants. For Classes I and III, the analysis of the F1 generation showed that the mutations were all non-allelic. A lack of complementation occurred only in Class II mutants (*bim*3, 4, 5, 6). The crosses between *bim*4-1 (*bim*40) and *bim*4-2 (*bim*70) and between *bim*5-1 (*bim*59) and *bim*5-2 (*bim*70) indicated that these pairs of mutants are allelic. Consequently, Class II contains 4 complementation groups (*bim*3 to *bim*6) (Table 3.I).

Time course of BMAA effects on germinating seedlings.

Previously, I have shown that the effect of BMAA on induction of hypocotyl elongation is specific to light-grown wild-type seedlings (Brenner et al., 2000). To further investigate this effect, the hypocotyl elongation of dark and light-grown seedlings in the presence or absence of 50μM BMAA was quantified at several points in time. Hypocotyl length measurements were taken from 3-, 4-, 5-, 6-, and 7 –day-old seedlings. In light-grown hypocotyls, the effect of BMAA is clearly visible after the

third day (Fig. 3.1A, *t*-test $P < 0.05$; *t*-test not shown). In the case of dark-grown etiolated hypocotyls, our measurements indicate that there is no significant difference between the mean values of the etiolated hypocotyl lengths between BMAA-treated and non-treated samples up to five days (Fig. 3.1B, 3.1C; *t*-test $P > 0.05$). On the sixth day and increasing on the seventh day, BMAA is slightly inhibitory as the mean length of the etiolated hypocotyls differs (Fig. 3.1B, 3.1C; *t*-test $P < 0.05$). These results suggest that BMAA does not have a specific effect on hypocotyl elongation in the dark but does have a general inhibitory effect in a time-dependent manner.

Gross position of *bim* mutants in the *Arabidopsis* genome

All the *bim* mutants were gross-mapped using PCR-based Simple Sequence Length Polymorphism (SSLP) (Bell and Ecker, 1994) and Cleaved Amplified Polymorphic Sequence (CAPS) (Konieczny and Ausubel, 1993) molecular markers polymorphic between Ler and Col ecotypes. One of the goals for gross-mapping the 10 different *bim* loci was proposed to determine whether these mutant loci co-segregate with any of the 20 *GLR* genes (Lacombe et al., 2001b) in the *Arabidopsis* genome. In fact, *bim*4 mapped near to *AtGLR* 3.4, but comparison of *bim*4-1 and wild type sequences revealed 100% identity with no nucleotide mismatches. Additionally, to determine if any of the isolated *bim* mutants had been previously characterized, complementation tests for those *bim* mutants that mapped near to the location of a previously described mutant were also performed. *bim3* mapped near *PROCUSTE*, (*PRC*) a cellulose synthase gene (Fagard et al., 2000). A complementation test performed between *bim3* and *prc* show allelism.

Map-based cloning of *bim4*

*bim*4-1was linked to the top arm of chromosome 1 and the mutation was localized to a single BAC, T20M3. Three SSLP markers developed within this BAC flanked *bim*4-1 within 42 kb NB8, and 7kb, NB9. A glycosyl hydrolase (chitinase like; *CTL*) gene lies within this interval (Fig. 3.2A). Considering the morphological and anatomical characteristics of *bim*4-1 (Fig. 3.3, 3.4), this gene was selected for sequencing from PCR products amplified from *bim*4-1 genomic DNA. The sequence was compared to the Col wild-type sequence from the GenBank database. The sequence analysis showed a G-to-A transition at the amino acid position 745; it changes the codon CGC to CAC, which transforms a conserved arginine in the *CTL*1 gene to a histidine (Fig. 3.2B). This transition revealed that the mutation in *bim*4-1 lies within a *chitinase-like* gene, named *AtCTL*1 or *ELP*1 (Zhong et al., 2002). In *elp*1, a mutant characterized by the ectopic deposition of lignin in pith, a G to A transition at nucleotide 701 changes the codon TGG to TGA. This transition transforms a tryptophan to a premature stop signal (Zhong et al., 2002) (Fig. 3.2B). The other allele of *bim*4, *bim*4-2, was also sequenced. Surprisingly, the sequence comparison between *bim*4-2 and wild type revealed that *bim*4-2 has the same point mutation as does *elp*1 (Fig. 3.2B). In the *bim* mutant, the fact that two point mutations were isolated within the same gene indicate that two separate mutations in the *AtCTL*1 gene are responsible for the *bim*4 phenotype. Henceforth *prc* will be referred to as *bim*3 and *ctl* as *bim*4.

Phenotype of *bim*3 and *bim*4

Figure 3.3 shows the phenotypes of the two alleles of *bim*3 and *bim*4 compared to wild type. *bim*3 has a phenotype similar to that of *bim*4 in all treatments, except that the

dark-grown hypocotyls of *bim*3 are slightly shorter (Table 3.1; Fig. 3.3B) and the roots of light-grown seedlings are slightly longer, but still shorter when compared to wild type (Fig. 3.3C). Roots in *bim*3 and *bim*4 are characterized by numerous, long hairs, which are slightly longer and more abundant in *bim*4 (Fig. 3.3C). In dark conditions, the hypocotyl length of *bim*3 and *bim*4 seedlings is decreased from 11% to 34% when compared to wild type and further decreased slightly by BMAA (Table 3.1, Fig. 3.3B). Thus, it appears that BMAA has a negative effect on hypocotyl length of these mutants in dark conditions.

Hypocotyl cross-sections show the effect of BMAA on wild type

To determine whether BMAA causes structural changes in the anatomy of elongated hypocotyls, cross sections from the hypocotyls of seedlings grown in the light or dark, and in the presence or absence of 50μM BMAA, were compared. Cross sections from etiolated seedlings of wild type show that there is no difference between the BMAA-treated and non-treated hypocotyls at the structural level (Fig. 3.4). This result supports the hypothesis that BMAA has no effect in the elongation of the dark-grown hypocotyl in wild-type plants at 50μM. However, when cross sections from BMAA-treated and non-treated light-grown hypocotyls were compared; there is the presence of large intercellular spaces and wavy cell walls in the BMAA-treated seedlings (Fig. 3.4B). An explanation for these observations is that the large intercellular gaps and the cell wall distortions are the result of the physical stress during the abnormal elongation process caused by BMAA.

bim3 and _bim4_ cause cell wall defects in the hypocotyl

As shown previously cross sections of wild-type seedlings grown in the light and BMAA have large intercellular spaces. In order to determine whether BMAA causes structural changes in the anatomy of light-grown hypocotyls of *bim*3 and *bim*4 mutants, cross sections of light- and dark-grown seedlings in the presence and absence of BMAA were performed. In light, in the absence of BMAA, *bim3* and *bim4* are similar to wild type with the exception of rare cell wall disruptions (Fig. 3.4). When grown in light plus BMAA, cell wall rupture and deformation in the hypocotyl are greatly increased, but the large intercellular spaces present in wild type are absent. Under dark conditions, as in wild type, there is no change between BMAA-treated and nontreated hypocotyls.

BIM3 and _BIM4_ are light-repressed genes

In order to understand whether there is a molecular response of *BIM3* and *BIM4* to the morphogenic effects of BMAA, I began by quantifying gene expression of *BIM3* and *BIM4* in light-grown plants compared to dark-grown plants (Fig. 3.5). Wild type plants were germinated and grown for 3 days in continuous darkness, and then either transferred to continuous light or kept in the dark for ten hours. The expression levels of *BIM3* and *BIM4* were measured relative to a reference gene, *eIF4A* (At3G13920) that encodes a putative eukaryotic initiation factor in *Arabidopsis thaliana*. *eIF4A* transcripts were used as a normalization control (levels remain unchanged in response to light; G.M. Coruzzi laboratory, unpublished data). When wild-type seedlings are treated in the light, mRNA levels of *BIM3* and *BIM4* are decreased to 39% as compared with dark-treated seedlings (Fig. 3.5). Although the two genes are repressed in samples grown in light - reaching maximum repression after ten hours of treatment (data not

shown) - it appears that they are always highly induced in dark conditions, regardless of treatment length. Interestingly, *BIM3* transcript levels are an order of magnitude lower than *BIM4* transcript levels indicating that *BIM4* may have broader domains of expression than *BIM3*.

Light regulation of *BIM3* and *BIM4* disrupted by BMAA

In order to determine the link between *BIM3*, *BIM4*, and BMAA, quantitative real-time PCR was similarly used to monitor the transcript abundance of *BIM3* and *BIM4* in the presence and absence of BMAA in wild-type plants. The expression patterns for *BIM3* and *BIM4* (Fig. 3.5) were similar under the conditions tested. Significant gene repression is observed in light-treated seedlings compared with dark-treated seedlings in the absence of BMAA as described above. However with the addition of BMAA, transcript levels for dark-treated seedlings are reduced by 37%, which are levels similar to light-treated seedlings. In illuminated plants, BMAA appears to slightly block light repression inducing the transcripts by 55% when compared to untreated plants. These sizable differences in the transcript values of dark- BMAA-treated versus BMAA-untreated samples indicate that BMAA represses *BIM3* and *BIM4* expression in dark conditions.

BMAA partially mimics light on a subset of genes in the dark.

In light conditions, it appears that BMAA represses photomorphogenesis by inducing hypocotyl elongation and inhibiting cotyledon opening. However, based on phenotypic and gene expression data described above, it also appears that BMAA has an effect in dark conditions. To understand the role that BMAA plays in dark conditions, I analyzed

the effects BMAA has on the expression of genes that are known to be induced either by light or dark: light induced genes *CAB* (chlorophyll a/b-binding protein; At3g47470; Zhang et al., 1991) and *GLN*2 (glutamine synthetase; At5g35630; Lam et al, 1998b; Oliveira and Coruzzi, 1999); and a dark induced gene, *ASN*1 (asparagine synthetase; At3g47340; Lam et al, 1998b; Oliveira and Coruzzi, 1999).

As previously described, quantitative real-time PCR was used to monitor the transcript abundance. The induction of *CAB* and *GLN*2 by light is reflected at the level of their gene expression (Fig. 3.6A). The low mRNA levels of *CAB* and *GLN*2 from dark-grown plants are elevated in light-adapted plants. In the dark, the presence of BMAA partially mimics the effect of light by causing a 100% induction of mRNA levels in *CAB* and 50% in *GLN*2 (Fig. 3.6A). In contrast *ASN*1, whose mRNA levels are induced in dark-grown plants (Fig. 3.6B) has no change in expression in the presence of BMAA (Fig. 3.6B). These results indicate that BMAA affects the expression of a subset of light regulated genes.

DISCUSSION

The *bim*3 and *bim*4 mutants were initially isolated in an attempt to identify GLR mutants in Arabidopsis by screening for insensitivity to morphogenic changes induced by BMAA, an animal iGluR agonist (Brenner et al. 2000). *bim*3 and *bim*4 are insensitive to BMAA-induced hypocotyl elongation. The basis of their mutant phenotype appears to be the suppression of cell elongation in the hypocotyl under light and dark conditions in the presence and absence of BMAA. Three *bim* mutants were studied, *bim*3 an allele of *prc*1; and two alleles of *bim*4: *bim*4-1, a missense allele,

which is a newly identified allele, and *bim*4-2, a nonsense allele identified previously as *elp*1, a mutant characterized by ectopic deposition of lignin in the pith and ethylene overproduction (Zhong et al., 2000).

Surprisingly, the defects of *bim*4 mutants result from a recessive mutation in the chitinase-like gene (*CTL*1) (Zhong et al., 2002) and those of *bim*3 mutants result from a recessive mutation in the cellulose synthase gene, *CeSA*6 (Fagard et al., 2000). The fact that chitinases are associated with plant defense and development and cellulose synthases with cell wall biosynthesis raises the significant question of whether CTL1 and CeSA6 are downstream targets of an *AtGLR* mediated light signaling pathway, or whether their role, seemingly essential for normal plant growth and development, is independent. In the latter case *bim*3 and *bim*4 would have been isolated from the BMAA screen only as an effect of the altered enzymatic activity of the mutant proteins.

To address this question, I investigated the expression of the two genes in *Arabidopsis* seedlings grown in the light or dark and in the presence or absence of BMAA. Light-grown plants show approximately a three-fold decrease in gene expression compared with dark-grown plants (Fig. 3.5). These findings indicate that *BIM*3 and *BIM*4 are normally light-repressed genes leading to photomorphogenesis; but in the dark they are induced and involved in the elongation of the hypocotyl (Fig. 3.7A). Repression of *BIM*3 by light has been previously reported by microarray analyses (Richmond and Somerville, 2001). Furthermore, the expression pattern of *PRC* (CeSA6) is reported in tissues undergoing expansion (Fagard et al., 2000).
In the light, BMAA causes the increase of transcript levels by 55% when compared with untreated plants (Fig. 3.5), indicating that BMAA partially de-represses *BIM*3 and *BIM*4 from light repression (Fig. 3.7B). The fact that BMAA counteracts light

repression of *BIM3* and *BIM4* is consistent with the hypothesis that these two genes are downstream targets of light signaling affected by BMAA. In this scenario GLR signaling may mediate the light regulation of *BIM3* and *BIM4*.

In contrast, in the dark-treated plants, BMAA partially mimics light by repressing the expression of normally dark-induced *BIM3* and *BIM4* (Fig. 3.5). To investigate the role of BMAA in dark conditions, I examined the effect of BMAA on mRNA expression of light regulated- (*CAB*, *GLN2*) and (*ASN1*) genes (Fig. 3.6). Interestingly those results indicate that BMAA partially mimics the effect of light in the dark-repression of *CAB* and *GLN2*, but has no effect on *ASN1*. In the BMAA-treated plants grown in the dark, the elevated expression of *CAB* and *GLN2* (Fig. 3.6) and the reduced expression of *BIM3* and *BIM4* (Fig. 3.5) indicate that BMAA partially mimics light to regulate a subset of genes affected in light signaling. It has been proposed that the photomorphogenic pathway represents the default route of development, whereas the etiolation pathway is an evolutionarily recent adaptation initiated by the angiosperms (Wei et al., 1994). On this basis, I postulated that the presence of BMAA is a plesiomorphy in Cycadales, a primitive group of gymnosperms, which synthesizes BMAA. In this scenario, BMAA functions to mimic light in dark conditions to affect light-regulated genes. Furthermore the fact that cycad plants (*zamia furfuracea*) grown in dark conditions up to two years developed up to 25 cm high in the total absence of light (data not shown) supports this hypothesis.

Ethylene signaling as a downstream target of AtGLR signaling

Induction of ethylene signaling has been observed in mutations for genes in cell wall biosynthesis as a consequence of altered wall composition (Ellis et al., 2002). *cev1*, a

constitutive expression VSP (vegetative storage protein) mutant (CeSA3), *bim*3 (CeSA6), and *bim*4 are mutants defective in cell wall. It has been reported that *bim*4 (*elp*1) and *cev*1 (CeSA3) constitutively produce ethylene (Zhong et al., 2002; Ellis et al., 2002). *bim*3 (CeSA6) may also constitutively express ethylene because it exhibits similar expression patterns as CeSA3 and both are expressed in cells undergoing expansion (Fagard et al., 2000; Scheible et al., 2001). The fact that the *cev*1 phenotype is partially suppressed by mutations that disrupt ethylene signaling (Ellis et al., 2002), suggests that disruption in ethylene signaling might also be responsible for the phenotypes of *bim*3 and *bim*4. How ethylene signaling and cell wall biosynthesis enzymes interact is an open question. Interestingly, ethylene signaling has been postulated to be coupled with Ca^{2+} fluctuations. Based on inhibition of different ethylene responses upon exposure to Ca^{2+} (Poovaiah & Leopold, 1973a,b), Knight et al. (1992) suggested a mechanism in which cytosolic Ca^{2+} fluctuations modify the expression of genes encoding biosynthetic enzymes of ethylene. The interaction between ethylene and Ca^{2+} in *Arabidopsis* root hair development also supports this view. Ethylene treatment inhibits root growth and increases root-hair number and length (Masucci and Schiefelbein, 1996; Zhong et al., 2002) whereas- Ca^{2+} signaling appears to be involved in root-hair growth (Wymer et al., 1997) possible mediated by depolarization-activated channels (Thion et al., 1998). That *bim4* constitutively expresses ethylene and shows an abnormal increase in root-hair number and length (Fig. 3.3C) could potentially indicate that Ca^{2+} modulation is disrupted in the mutant. In this scenario, disruption of ethylene signaling and abnormal root hairs in *bim*4 could be either directly a result of a disruption in Ca^{2+} signaling possibly mediated by *AtGLRs* or indirectly a result of the altered enzymatic activity of the mutant protein, assuming these

are downstream targets of the GLR signaling affected by BMAA.

An alternative hypothesis is that *BIM4* a chitinase can be regulated by GLRs in response to stress. Kinnersley & Turano (2000) speculate that environmental stresses like pathogenic elicitors on plants trigger the activation of GLRs. A number of studies have provided evidence for the pivotal role of cytosolic Ca^{2+} fluctuations and thus the involvement of ion transporters in triggering plant defense responses upon pathogen exposure (Dixon et al., 1994; Ebel and Scheel, 1992).

I postulate for example that BIM3 and BIM4, whose mutated proteins appear to confer insensitivity to the elongation of the hypocotyl by BMAA as a result of cell wall defects, are downstream targets of a signaling disrupted by BMAA. *BIM3* and *BIM4* have specific functions that directly or indirectly play a role in plant development. However, *plant development* is a general term that comprises a network of pathways in the organism as a whole.

MATERIALS AND METHODS

Plant Growth Conditions

Surface-sterilized *Arabidopsis* seeds mutagenized with ethyl methane-sulfonate (Lehle Seeds, Round Rock, TX) were plated on Murashige and Skoog (Sigma) medium supplemented with 1% sucrose, and 8% agar. pH was adjusted to 5.7 before addition of agar. A final concentration of 50μM BMAA (Sigma) was added to the medium. Seeds were pretreated for 3 days at 4°C, before growing them vertically in square plates (100 x 15mm) for 7 days. White light at 70μE m^{-2} s^{-1} was used for all treatments. For the dark treatment seeds were plated and light pretreated before they were grown in the dark for

5 days. Selected M2 plants that showed resistance to BMAA were grown in Metromix 200 (Grace, Sierra) in a 16-h light/8-h dark cycle at 22°C in a plant growth chamber.

Genetic mapping

For genetic mapping, mutants (Col background) were backcrossed four times before outcrossing to Ler ecotype to generate a mapping population. The resulting F1 plants were selfed and the F2 seed was plated on medium containing 50μM BMAA. Small leaves from mapping plants were selected for isolation of genomic DNA.

Analysis of DNA

Arabidopsis genomic DNA for mapping analysis was isolated according to the procedure described by Edwards et al. (1991). *Arabidopsis* genomic DNA for sequencing analysis was isolated using a modified version of Shure, et al., (1983). Primer to sequence the coding region of *AtCTL1* (At1g05850) are: 5'-ACTTGAGAGCAACGGCGATA-3', 3'-TCAAGCTGTTGGTTTCTGGG-5'; 5'-TGCTCAATGTACTCAGGGTGGT-3', 3'- CCAATGCAATCCTACTGTGAC-5'; 5'-CTGTTGTAGCACAGACCCCAAG-3', 3'- CTTCCTTATTTTCTCGGCAACG-5'

Design of SSLP and CAPS markers for genetic and physical mapping.

New SSLP and CAPS markers were designed using the Cereon Arabidopsis Polymorphism and Ler sequence collection from the TAIR database. Small DNA sequences (150-300bp) including the Insertion Deletions or Single Nucleotide Polymorphism of interest were downloaded from GenBank.

Histology

One week-old plant tissue was fixed in 4% paraformaldehyde in PBS (Phosphate-buffered saline) overnight at 4°C, followed by rinsing in PBS, twice. The tissue was subsequently pre-embedded in 1% agarose, dehydrated in an ethanol series, and infiltrated with Historesin (Technovit 7100, Kulzer). 5μm sections were cut with a microtome mounted and stained by submersion in 0.05% toluidine blue for 3 min.

RNA quantification

Total RNA was isolated using the RNeasy Mini Kit (Qiagen). One microgram of RNA was reverse-transcribed with 15 u of reverse transcriptase using 0.5μg Oligo-dT according to the manufacturer (Promega).

Primers for RT-PCR

Desalted primers covering specific and unique regions were generated. The sequences were downloaded from the TAIR database. Primers spanned at least one intron for each of the genes. *CTL*1: 5'-ACTTGAGAGCAACGGCGATA-3', 3'-CCAATGCAATCCTACTGTGAC-5'; *PRC*1: 5'-TGGAGAACCGTTTGTGGCATGT-3', 3'-TCGGGTCAGAAAGAGAAACAGGAT-5', covering the N-terminal region specific for each CeSA (position 170- 553); eIF4A: 5'-TGATACTAGTACGGCAGAGC-3', 3'-ATCACCACTGACCTCTTAGC-5'. For amplification and detection of *ASN*1, *CAB* and *GLN*2 the following primers and probes were used: *ASN*1: 5'-TCACGCTGCTCAAAATGT-3', 3'-GAGTGGGATGCAAGCT-5', 5'-AGAACTCTGCGAGACTAACGG-3' (anchor probe), and 3'-

CGGTGGCACCTCCAGG-5' (sensor probe); *CAB*, 5'-TGGTCACGCCACAATC-3', 3'-CCGTAACACTCTCTTTTCCT-5', 5'-ACACCCAAGTGAGACAACGAA-3' (anchor probe), and 3'-ATTCACCTCCCCATAACCCT-5' (sensor probe); *GLN2*, 5'-AGCTAGTATTGACCAGTTCT-3', 3'-CTGAAGCCCTTGCAGC-5', 5-AACCGTGGATGCTCTATTCGT-3' (anchor probe), and 5'-CCTCGGTGTCACGTCCC-5' (sensor probe). Anchor probes were labeled at the 3' end with fluorescein, and sensor probes were labeled at the 5' end with LC-Red 640 and phosphorylated at the 3' end.

LightCycler real-time PCR

For LightCycler reactions, a master mix of the following reaction components was prepared to the indicated end concentration: 10µl water, 2.4µl $MgCl_2$ (25mM), 1.8 µl forward primer (10mM), 1.8 µl reverse primer (10mM) and 2.0 µl LightCycler (DNA Master SYBR Green I; Roche Diagnostics). LightCycler mastermix (18µl) was filled in the LightCycler glass capillaries and 2 µl cDNA was added as template. All templates were amplified using the following LightCycler protocol: denaturation incubated at 95°C for 2 min, the template was amplified and quantified for 36 cycles (95°C for 0 sec, 58°C for 10 sec, 72°C for 15 sec with a single fluorescence measurement). After 40 cycles a melting curve was generated with the following program: 95°C for 0 sec followed by 50°C for 5 sec and a slow heating rate of 0.1°C per second to 95°C with continuous fluorescence measurement and a final cooling step of 40°C for 30 sec. Standars were prepared with a 10-fold serial dilution (10^{-4} to 10 pg) of the PCR products and were run under the same PCR conditions used for the samples, The

amount of CTL1, PRC1, ASN1, GLN2, and CAB was corrected/normalized according to the amount of At3G13920.

Statistical significance

A *t*-test was applied to the data samples to investigate the significance of the results. I tested if the mean of two measurements (one pair), differ significantly at the 95% confidence level.

Table 3.1. Genotype and phenotype of the 10 isolated *bim* mutants.

Class			WT	I		II						III	
***bim* mutant number**			**WT**	**131**	**175**	**18**	**40**	**77**	**59**	**136**	**167**	**26**	**50**
***bim* allele**				*bim1*	*bim2*	*bim3*	*bim4-1*	*bim4-2*	*bim5-1*	*bim5-2*	*bim6*	*bim7*	*bim8*
Hypocotyl Length (mm)	Light	+BMAA	6.7 +/-0.8	2.7 +/-0.5	3.3 +/-0.5	3.3 +/-0.6	2.6 +/-0.4	2.4 +/-0.4	2.5 +/-0.5	2.7 +/-0.6	2.1 +/-0.4	1.7 +/-0.3	2.1 +/-0.3
		-BMAA	2.4 +/-0.4	1.5 +/-0.5	2.5 +/-0.1	2 +/-0.2	2.3 +/-0.3	2.1 +/-0.3	1.8 +/-0.2	2 +/-0	1.1 +/-0.2	2.6 +/-0.3	2.1 +/-
	Dark	+BMAA	21 +/-1.9	19 +/-1.3	20 +/-2.7	2.5 +/-0.4	4.4 +/-0.7	5.8 +/-0.4	11.6 +/-2.7	10.8 +/-0.9	12.7 +/-1.6	7.8 +/-1.3	6.7 +/-1.4
		-BMAA	20.9 +/-1.9	19.9 +/-1.4	20 +/-2	2.5 +/-0.8	6.9 +/-0.9	7.4 +/-0.7	12 +/-1.8	11.5 +/-1.2	14.5 +/-1.7	9.6 +/-1	8.2 +/-1.8

The hypocotyl length number represents the mean and the +/- represent SD of >30 individuals.

Figure 3.1. Quantification of Hypocotyl lengths of wild-type seedlings grown in the light or in dark in the presence or absence of 50μM BMAA.

(A) Mean hypocotyl lengths of light-grown seedlings over time (days).

(B) Mean hypocotyl lengths of dark-grown seedlings over time (days).

(C) *t*-test analysis of hypocotyl lengths grown with or without BMAA at 3, 4, 5, 6, and 7 days. (probability<0.05). The data represent the mean and SD of > 30 individuals. ts, statistical sample.

A

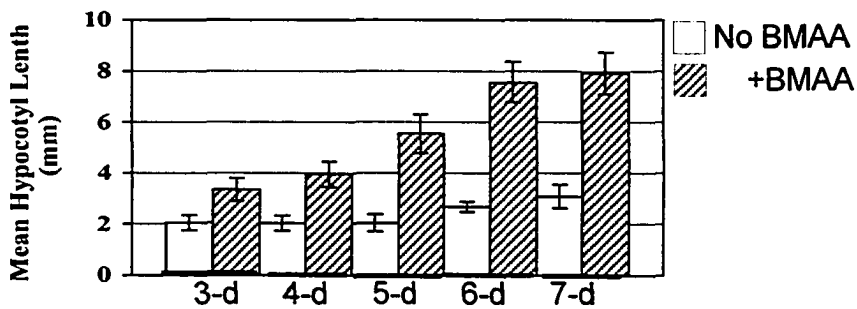

B

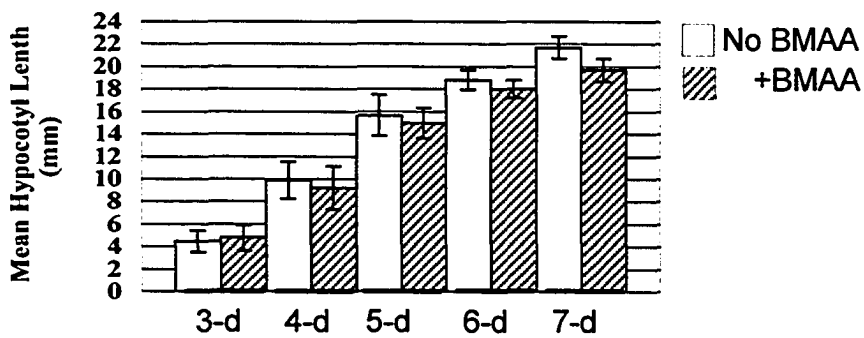

C

Days	Comparison (dark)	ts	t0.05[*df*]	*t*-test	Mean hypocotyl length
3	3d (-) vs 3d (+) BMAA	0.5	2	P > 0.05	similar
4	4d (-) vs 4d (+) BMAA	1.1	2	P > 0.05	similar
5	5d (-) vs 5d (+) BMAA	1.4	2	P > 0.05	similar
6	6d (-) vs 6d (+) BMAA	2.6	2	P < 0.05	different
7	7d (-) vs 7d (+) BMAA	4.3	2	P < 0.05	different

Figure 3.2. Positional cloning of the *BIM4* locus. SSLP and CAPS markers were used to fine-map the *bim*4 locus within an interval of 64 kb on BAC T20M3. NB molecular markers are deposited in TAIR.

(A) Physical map of the region of chromosome 1 containing the CTL gene. Name within the BAC indicates the molecular marker used in that position.

(B) Scheme of the *bim4* mutations in the *AtCTL1* gene. Both mutations are transitions from G to A indicated by an asterisk at nucleotide 701 and 745.

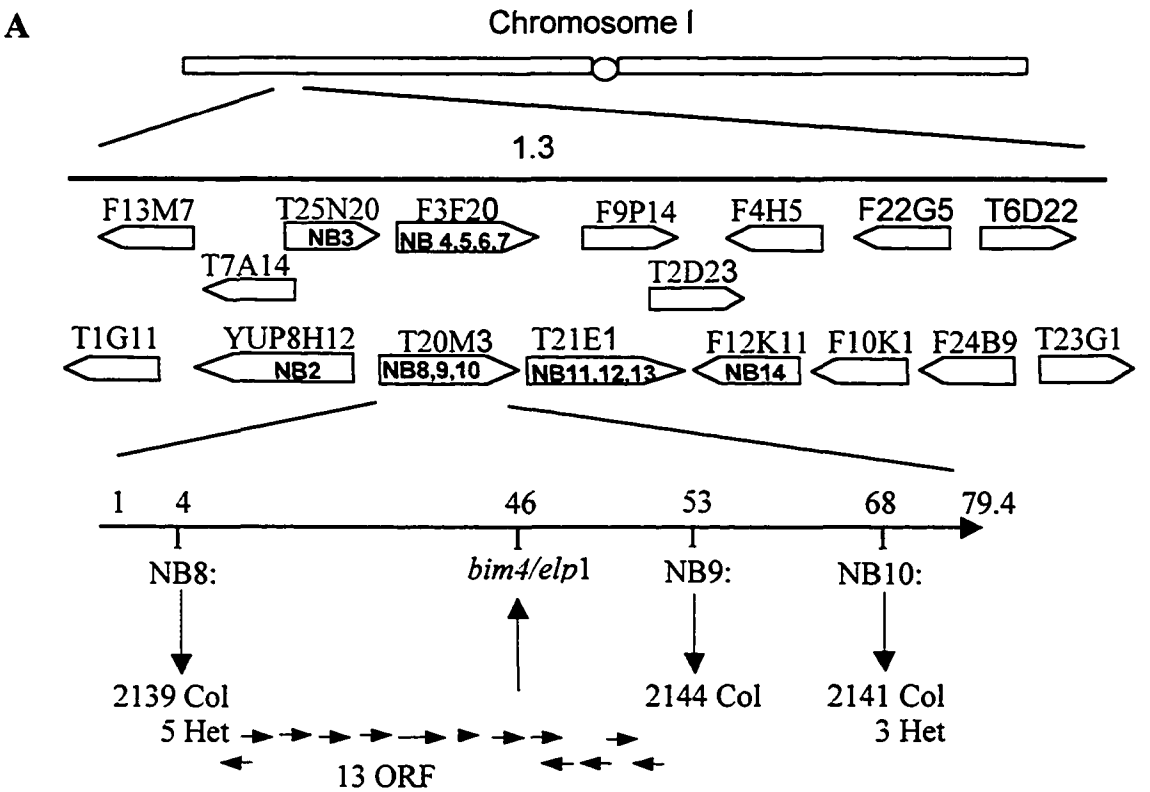

B

*elp*1

701 745

WT TGGAAATTCAAGTACCCCTGCAGCCCTGGAGCTGAATACTACGGACGC

CTL protein W K F K Y P C S P G A E Y Y G R

bim4 TGAAAATTCAAGTACCCCTGCAGCCCTGGAGCTGAATACTACGGACAC

CTL protein stop K F K Y P C S P G A E Y Y G H

Figure 3.3. Phenotypic analysis of *bim3* and *bim4* mutants.

(A) M3 seed grown in the light on MS medium plus and minus BMAA.

(B) M3 seed grown in the dark on MS plus and minus BMAA. The seed was exposed to light for 4 hours to stimulate germination before grown in the dark for 7 days.

(C) Close-up of *bim3* and *bim4* root in the light on MS medium. Scale bar, 2mm.

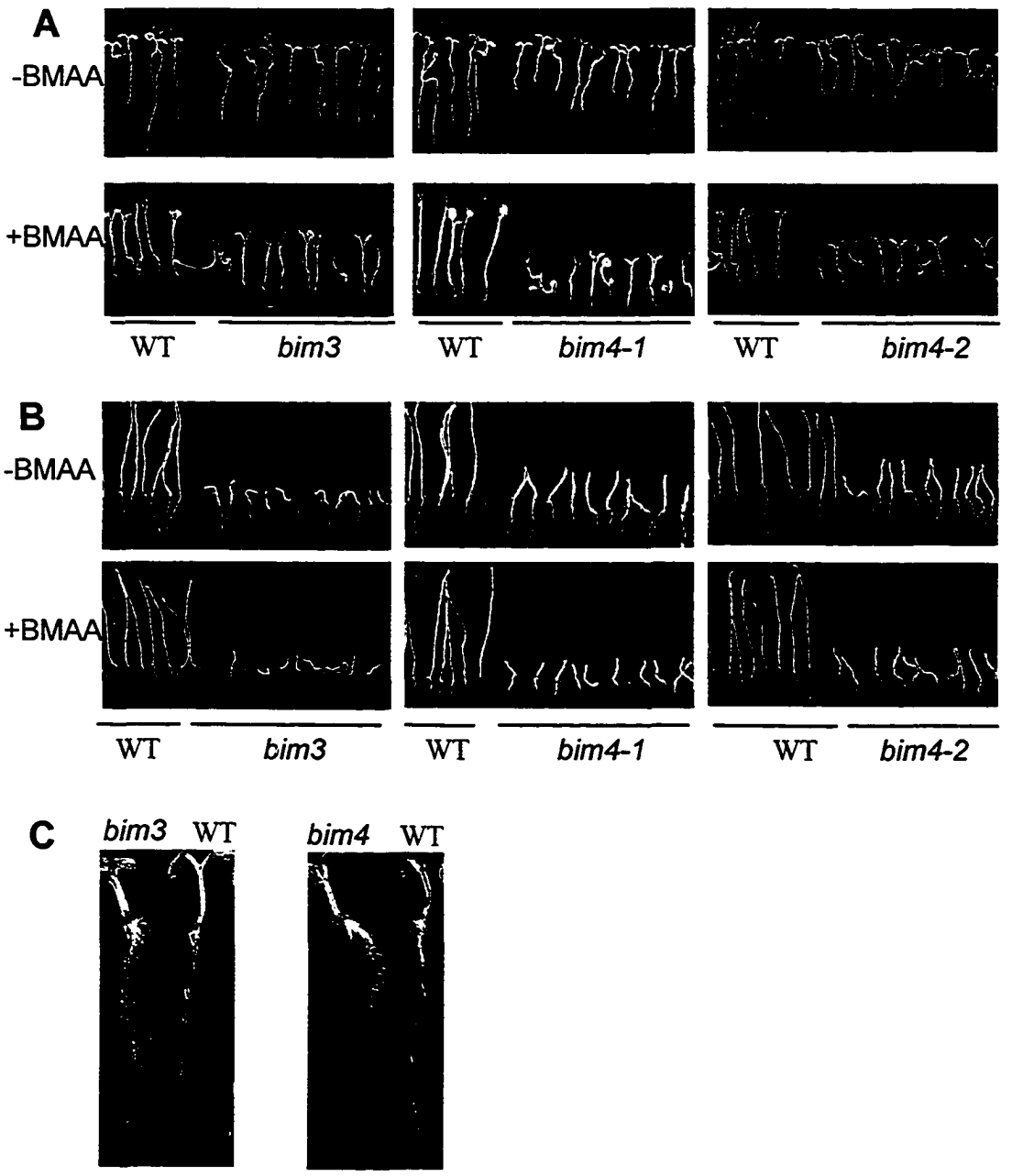

Figure 3.4. Effect of BMAA in cross sections of light and dark-grown hypocotyl of wild type compared to *bim3* and *bim4* mutants.

(A) Anatomical cross sections show no difference between BMAA-treated and nontreated etiolated seedlings. The dark-grown samples shown, represent sections in the presence of BMAA. Arrow heads in the cross section of wild type in light plus BMAA points to large intercellular spaces in the cortex. Arrows indicate cell wall rupture. **(B)** Close-up of the intercellular space in BMAA-treated, light-grown wild-type hypocotyls.

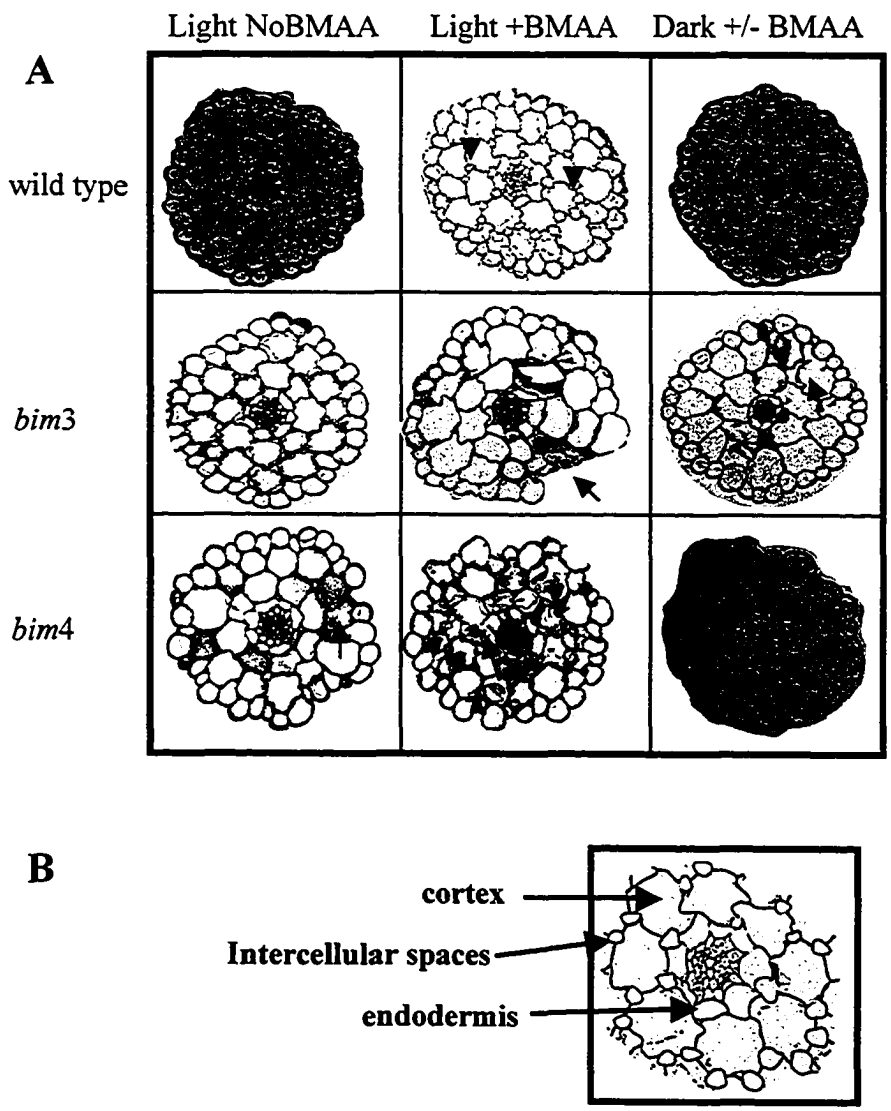

Figure 3.5. Quantification of gene expression of *BIM3* (*PRC*) (A) and *BIM4* (*CTL*) (B) in the presence and absence of BMAA in wild-type seedlings. Three day etiolated-grown seedlings transferred to 50μM BMAA in maintained either in continuous darkness (diagonal bars) or illuminated for 10 hrs. All transcripts were measured using real-time quantitative PCR and normalized to a putative eukaryotic initiation factor 4A (AT3G13920). The data represent the mean and Standard Deviation of 4 separate experiments.

A

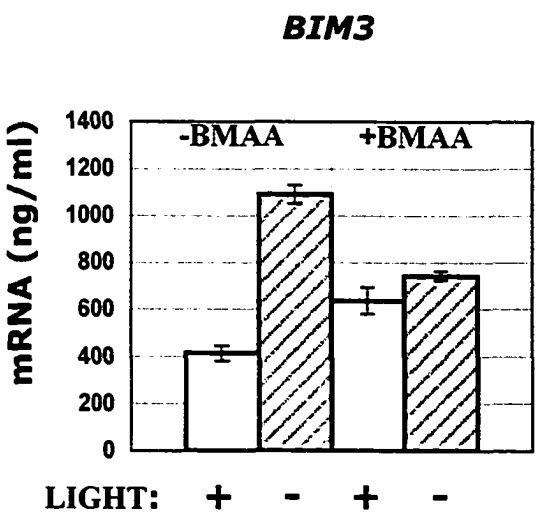

B

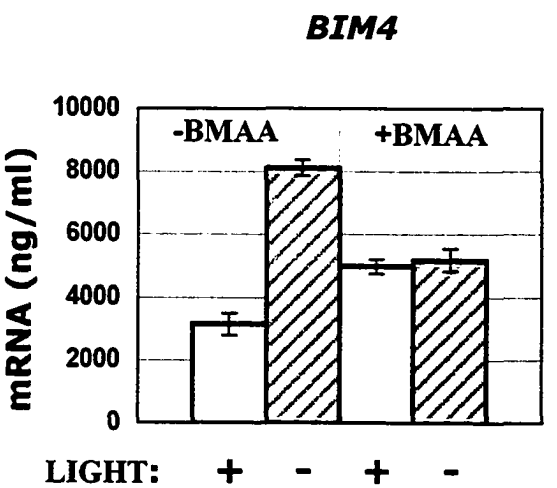

Figure 3.6. In the dark BMAA partially mimics light on a subset of genes. All transcripts were measured in 3-day etiolated wild-type seedlings. After transfer to 50μM BMAA and maintained in continuous darkness (diagonal bars) or illuminated for 10 hrs. **(A)** BMAA can partially mimic the effect of light by causing the induction of *GLN*2 and *CAB* transcripst in dark conditions.

(B) BMAA has no effect on the expression of *ASN*1, a gene induced by dark conditions. Transcripts were measured using real-time quantitative PCR and normalized to a putative eukaryotic initiation factor 4A (AT3G13920). The data represent the mean and standard deviation of four separate experiments.

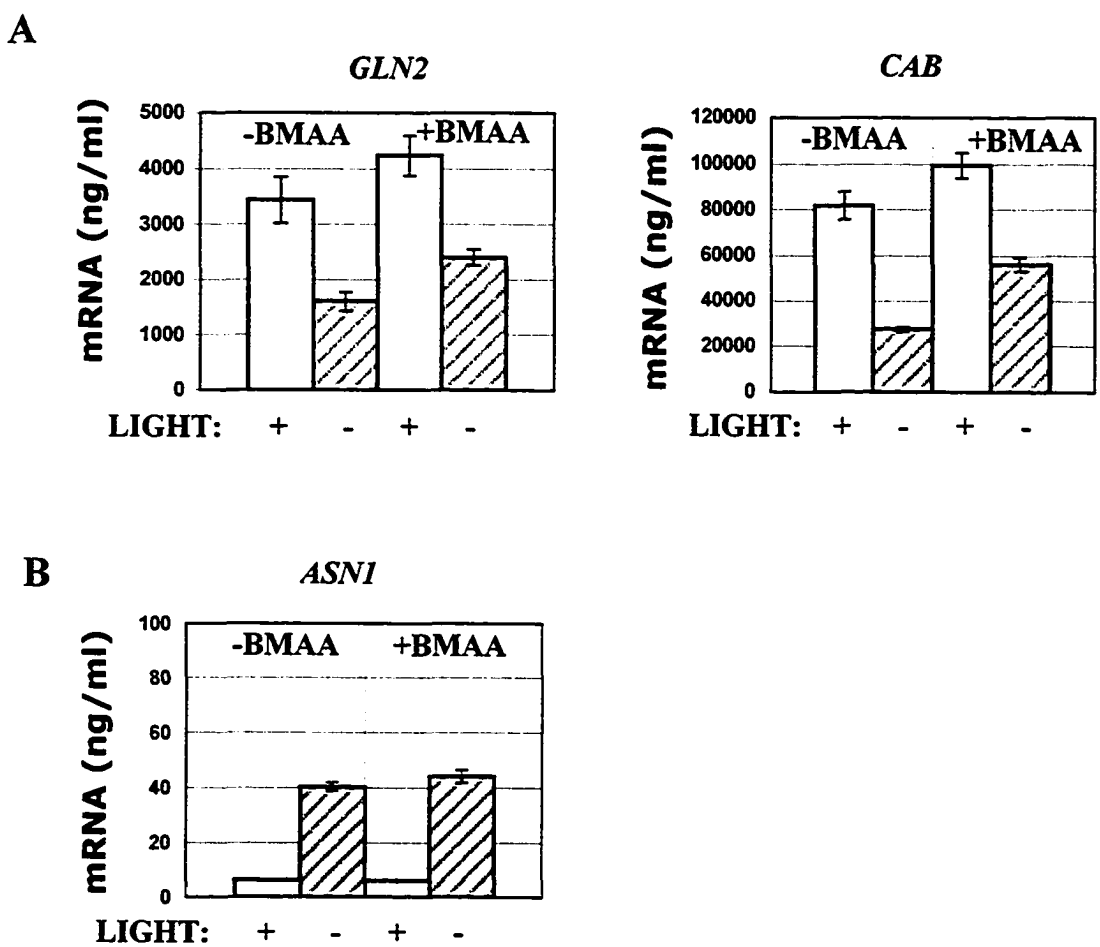

Figure 3.7. A proposed model representing the effect of BMAA on *BIM3* (*PRC*) and *BIM4* (*CTL*).

(A) In the light *BIM3* and *BIM4* are normally repressed. While in the dark, the induction in their transcript levels indicate their involvement in cell elongation.

(B) In the presence of BMAA in the light, *BIM3* and *BIM4* are specifically de-repressed leading to elongation of hypocotyl. But in the dark, BMAA partially mimic light repression. This repression has no observable effect on the phenotype of the etiolated seedling.

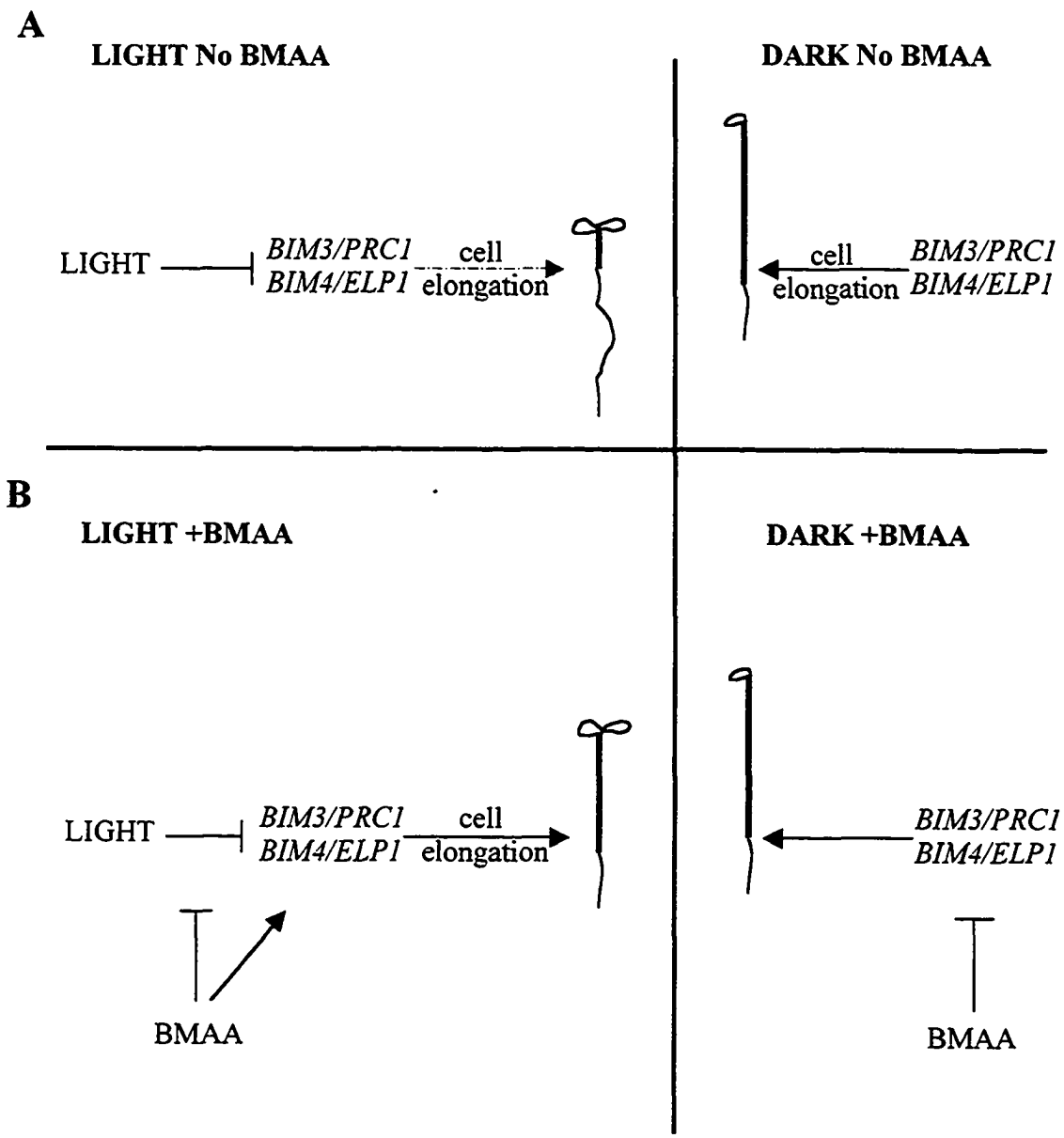

Appendix to

Chapter 3

This appendix contains additional background information related to chapter 3, which will be submitted as a publication to the Journal The Plant Cell.

RESULTS

Design of New SSLP and CAPS molecular markers to clone *BIM4*

New SSLP and CAPS molecular markers were designed by using SNP and INDELs polymorphism from the Cereon *Arabidopsis* Polymorphism and Ler sequence collection from the TAIR database. Figure A-3.1, shows the 21 molecular markers that were designed for the mapping of *bim4* and submitted to the TAIR (The Arabidopsis Information Resource) database.

Positional cloning of the *BIM4* gene

To generate a new mapping population, introgressed individuals which were recombinants in T23G18 (two plants with a heterozygous and one with a Landsberg genotype) and T1G11 (four plants with a heterozygous genotype) were used (Table A-3.1). The aim was to increase the crossing-over event within the mapping region and therefore to increase the number of recombinants. Seed from these introgrossed F2 mapping plants, was plated on media and "F3 families" were grown. A few Landsberg introgressed mutants from each "F3 family" were crossed to Landsberg plants to generate the new F1 population.

Table A-3.1. Introgressed plants used to create a new mapping population to achieve the mapping of *BIM4*.

F3 recombinant individuals introgressed into the Ler	Genotype in BAC T1G11	Genotype in BAC T21G18
*bim*4 T-4	Heterozygous	Col
*bim*4 T-10	Heterozygous	Heterozygous
*bim*4 T-23	Ler	Col
*bim*4 T-24	Col	Heterozygous
*bim*4 T-46	Col	Heterozygous
*bim*4 T-47	Col	Heterozygous

Upon harvesting, the new introgressed F1 seed was grown and plants were selfed. The F2 seed derived was plated on medium containing 50μM BMAA. From this population a total of 1944 F2 *bim* mapping plants were selected and isolated. The DNA from these individual was amplified with SSLP and CAPS markers within the minimal interval. Typically, a few plants are incorrectly screened, thus providing false information. Therefore every recombinant within the region was additionally progeny-tested to confirm the *bim/bim* genotype. Figure A-3.2, shows the distribution of the recombinants derived from the cross between the *bim*4 mutants introgressed into the Ler background with Ler wild-type plants. Five recombinants border the left side of the minimal interval and 3 recombinants border the right side. A total of 27 informative recombinants were found within the highly introgressed mapping population of 1944 individuals. Interestingly, from the five original introgressed *bim*4 F2 individuals

crossed to Ler (Table A-3.1) only the population derived from *bim*4 T-10 provided the largest number of recombinants. *bim*4 T-10 is heterozygous on both sides of the minimal interval and in a population of 280 individuals, 12 informative recombinants were identified.

Gene identification

The genomic sequence of the *BIM*4 gene encodes a member of the glycosyl hydrolase family 19 (chitinase). The gene is located in chromosome 1, on the assembly T20M3. Its locus name is T20M3.12/At1g05850 (Fig. A-3.3). The gene length is 1285 bases and contains three exons and two introns. The three exons are located between nucleotide residues 1 to 388, 607 to 766, and 868 to 1285. Its predicted protein length is 322 residues (Fig. A-3.4). O-glycosyl hydrolases are a widespread group of enzymes that hydrolyze the glycosidic bond between two or more carbohydrates, or between a carbohydrate and a non-carbohydrate moiety. Glycosyl hydrolases are classified into 85 different families based on sequence similarity. *bim*4 belong to the glycoside hydrolase family 19, composed of enzymes with only one known activity: chitinase. In plants, these enzymes function in the defense against fungal and insect pathogens by destroying their chitin-containing cell wall. Chitinases are enzymes that catalyze the hydrolysis of the β-1,4-N-acetyl-D-glucosamine linkages in chitin polymers.

Calibration curve analysis for real-time RT-PCR

Absolute quantification uses a calibration curve analysis (external standard) to normalize a target gene with an endogenous standard. The standard or control genes are

mainly non-regulated reference genes. These are present in all nucleated cell types and are involved in basic cell functions. Calibration curves were created for the control gene (*eIF*4A) and for the two genes of interest, *PRC1* and *CTL1* (Fig. A-3.5)

To create the calibration curve reports, primer specificity of RT-PCR products was documented with gel electrophoresis. These resulted in single products (*CTL1*, 503bp; *PRC1*, 379bp; and *eIF4*, 296bp). No primer-dimers were generated during the applied 40 real-time PCR amplification cycles. Once the PCR fragments were purified, serial dilutions with known concentrations were used to generate the standard curve or calibration curve report. Having a standard curve for each gene, the crossing points of unknown samples are determined (from the light cycler report) and the corresponding concentrations are automatically calculated. A *t*-test shows that for typical CP values between 15 and 20 there is a ~5% uncertainty in the resulting cDNA concentration due to statistical variations of the slope of the regression curve at a 95% confidence levels.

Real-Time RT-PCR absolute values

Plotting the crossing points (CP) of the individual samples in the LightCycler analysis report versus the logarithm of the cDNA concentration allows to determine absolute values, which are used to quantify the gene transcript (Fig. A-3.6). The CP is defined as the point at which the fluorescence starts to rise above the background fluorescence, or at which PCR amplification begins its exponential phase. The CP for each sample at a given cDNA concentration is taken from the analysis setting report (Fig. A-3.6).

The intercept of the linear regression of the data in the curve analysis is subtracted from each measured CP value from the analysis report, and the result is divided by the slope of that curve. This procedure is done for the gene of interest and for the control gene. The figures for the absolute quantification are then given by the ratio between the gene of interest/control gene.

Figure A-3.1. SSLP and CAPS markers designed to map *bim*4. The markers were generated using the Cereon polymorphism database. PCR primers were designed on a DNA sequence containing the sought polymorphism, which was downloaded from GenBank. The markers are deposited in TAIR.

Marker Name	Chrom.	Marker Type	PolymorphismType	Fragment Length
NB1	1	SSLP	INDELs	Col 237; Ler 189 bp
NB2	1	SSLP	INDELs	Col 300; Ler 331 bp
NB3	1	SSLP	INDELs	Col 146; Ler 134 bp
NB4	1	SSLP	INDELs	Col 236; Ler 259 bp
NB5	1	SSLP	INDELs	Col 199; Ler 215 bp
NB6	1	CAPS	SNP	Col 0.732, Ler 0.217;0.509 kb
NB7	1	CAPS	SNP	Col 0.222; 0.510, Ler 0.732 kb
NB8	1	SSLP	INDELs	Col 122; Ler 113 bp
NB9	1	CAPS	SNP	Col 0.406; 0.255, Ler 0.662
NB10	1	CAPS	SNP	Col 0.222; 0.473, Ler 0.776
NB11	1	CAPS	SNP	
NB12	1	CAPS	SNP	Col 0.800; Ler 0.685;0.115
NB13	1	CAPS	SNP	Col 0.590; Ler 0.362;0.220
NB14	1	SSLP	INDELs	Col 179; Ler 134 bp
NB15	1	SSLP	INDELs	Col 103; Ler 91 bp
NB16	5	SSLP	INDELs	Col 251; Ler 167 bp
NB17	5	SSLP	INDELs	Col 128; Ler 112 bp
NB18	5	SSLP	INDELs	Col 174; Ler 102 bp
NB19	2	SSLP	INDELs	Col 170; Ler 104 bp
NB20	2	SSLP	INDELs	Col 1037; Ler 971 bp
NB21	2	SSLP	INDELs	Col 246; Ler 268 bp

SSLP: Simple Sequence Length Polymorphism

CAPS: Cleaved Amplified Polymorphic Sequence

INDELs: Insertion Deletions

SNP: Single Nucleotide Polymorphism

Figure A-3.1. Continued

Marker Name	PCR Primer Sequence I	PCR Primer Sequence 2
NB1	gaaaccaacccaagattagtaaaa	gcgaagaaccactaaaccctaatca
NB2	ccatatacgaagcccagaaacaaa	cctcctcttccttcttcgtactctc
NB3	cccgtcacttcaaagccccc	aataacctcaaaaagggaacataaagatgat
NB4	cgtcgagagtaagaactctgactagaaa	ggcagaaggcggagactttgaa
NB5	tcatcttccctgagagagagaca	gttgtcgaagtagtctttttttccca
NB6	tttgatggtgatttgactttgc	tcagattggctcaagtaaacga
NB7	ttcccgttgctaaatctcaaca	aggagattgatgcgagaagtcc
NB8	ctgaactgttgttcgtgattccaa	ttgaactgcccacatgagtacataaca
NB9	ttgagatgctggagttgacg	ttgaagaagaccaagtcgttga
NB10	cggctgagagaaacacgatg	cgcacctaaacgcccaaagacag
NB11	gaggcagtcttggggagaaga	tggatctgattggcggtgata
NB12	ggaggacttgaagaggctga	gcctcgtctccaaaatgaaa
NB13	cagtcttggtttaggctcgtct	tgacagggacaaaacaacaaag
NB14	gcctgtcaccaactacgtaac	ttctcgaatctaaccaaatgtctt
NB15	atgctttggttgtgtgaataatt	agtttctctcctacgctcttcatt
NB16	tactcctctaagcattccata	cctttgcttaccacacttagat
NB17	ttcactttgaccgttactctg	atgccttggagagtgagaaa
NB18	taaggtagcttgggacga	catccatgaacctttgcttgtc
NB19	aacaacctttgagcagagttacc	tgcagggaagagaaaaggaaatag
NB20	actgggtggagtaccagaacaa	accaagaaagcgagaaagacgag
NB21	ctaaacccagagaagcaaaatc	acagcttcctccgtcaactac

Figure A-3.1. Continued

Marker Name	Enzyme	Ecotype	Map Name	map_ location start	map_ location end
NB1		Col-0;Ler	AGI_clone:F10O3	705770	705818 bp
NB2		Col-0;Ler	AGI_clone:yUP8H12	1527301	1527302 bp
NB3		Col-0;Ler	AGI_clone:T25N20	1640760	1640772 bp
NB4		Col-0;Ler	AGI_clone:F3F20	1679086	1679087 bp
NB5		Col-0;Ler	AGI_clone:F3F20	1705029	1705030 bp
NB6	SspI	Col-0;Ler	AGI_clone:F3F20	1709823	1709825 bp
NB7	DraI	Col-0;Ler	AGI_clone:F3F20	1721335	1721337 bp
NB8		Col-0;Ler	AGI_clone:T20M3	1725741	1725750 bp
NB9	BstNI	Col-0;Ler	AGI_clone:T20M3	1775173	1775175 bp
NB10	NsiI	Col-0;Ler	AGI_clone:T20M3	1800015	1800017 bp
NB11	BsmAI	Col-0;Ler	AGI_clone:T21E18	1815899	1815901 bp
NB12	AciI	Col-0;Ler	AGI_clone:T21E18	1850604	1850606 bp
NB13	BfaI	Col-0;Ler	AGI_clone:T21E18	1868932	1868934 bp
NB14		Col-0;Ler	AGI_clone:F12K11	2017030	2017075 bp
NB15		Col-0;Ler	AGI_clone:F4H5	2073468	2073481 bp
NB16		Col-0;Ler	AGI_clone:MUB3	25417010	25417095 bp
NB17		Col-0;Ler	AGI_clone:MJE7	19272260	19272277 bp
NB18		Col-0;Ler	AGI_clone:MYH19	15571833	15571906 bp
NB19		Col-0;Ler	AGI_clone:F3K23	9056917	9056918 bp
NB20		Col-0;Ler	AGI_clone:F3K23	9117180	9117247 bp
NB21		Col-0;Ler	AGI_clone:F2G1	9207286	9207287 bp

AGI: Arabidopsis Genome Initiative

Figure A-3.2. F2 informative recombinants used to fine mapp *bim*4. Marker NB2 is located in the YAC YUPH18, NB3 in BAC T25N3, and NB14 in BAC F12K11. The total distance between NB2 and NB14 is 1.3 Mb

	——F3F20——						—T20M3—		—T21E1 ——				
Recombinants	NB2	NB3	NB4	NB5	NB6	NB7	NB8	NB9	NB10	NB11	NB12	NB13	NB14
24A-23	C	C	C	C	C	C	C	C	C	C	C	C	H
24A-40	H	H	C	C	C	C	C	C	C	C	C	C	C
24A-45	C	C	C	C	C	C	C	C	C	C	C	C	H
24A-132		H	C	C	C	C	C	C	C	C	C	C	C
24A-336	C	C	C	C	C	C	C	C	C	C	C	C	H
24B-87	H	H	H	H	H	H	H	C	C	C	C	C	C
24C-17	H	H	H	H	H	H	H	C	C	C	C	C	C
24C-35		C	C	C	C	C	C	C	C	C	C	C	H
24C-48	H	H	H	H	H	H	H	C	C	C	C	C	C
24C-51	C	C	C	C	C	C	C	C	C	C	C	C	H
24C-296	H	H	H	H	H	H	H	C	C	C	C	C	C
24C-339	C	C	C	C	C	C	C	C	C	C	C	C	H
24C-495	C	C	C	C	C	C	C	C	C	C	C	C	H
24C-560	H	H	H	H	H	H	H	C	C	C	C	C	C
24C-666	C	C	C	C	C	C	C	C	C	C	C	C	H
10A-66	C	C	C	C	C	C	C	C	H	H	H	L	L
10A-94	C	C	C	C	C	C	C	C	H	H	H	L	L
10A-193	C	C	C	C	C	C	C	C	H	H	H	L	L
10A-255	C	C	C	C	C	C	C	C	C	C	H	H	L
10A-256	C	C	C	C	C	C	C	C	C	C	H	H	L
10A-259	C	C	C	C	C	C	C	C	C	C	H	H	L
10A-261	C	C	C	C	C	C	C	C	C	C	H	H	L
10A-269	C	C	C	C	C	C	C	C	C	C	H	H	L
10A-271	C	C	C	C	C	C	C	C	C	C	H	H	L
10A-274	C	C	C	C	C	C	C	C	C	C	H	H	L
10A-275	C	C	C	C	C	C	C	C	C	C	H	H	L
10A-277	C	C	C	C	C	C	C	C	C	C	H	H	L

Figure A-3.3. Genes in BAC T20M3. This BAC is 7943- bp long. The locus name and the 5' to 3' direction are in an ascendant order.

Locus	5' -3'	Gene product name
At1g05750	24-1526	Pentatricopeptide (PPR) repeat-containing protein
At1g05760	2941-2298	Jacalin lectin family (RTM1)
At1g05770	4751-4048	Jacalin lectin family
At1g05780	5262-6681	Unknown protein
At1g05785	9482-10907	Unknown protein
At1g05790	11540-15706	Putative NPK1-related protein kinase 2
At1g05800	19705-21120	Hypothetical protein
At1g05805	23344-25928	bHLH protein
At1g05810	26944-27851	RAS-related GTP-binding protein (ARA-1)
At1g05820	28277-32268	Unknown protein
At1g05830	32962-41203	Unknown protein
At1g05840	44651-41344	Expressed protein
At1g05850	46618-45334	Glycosyl hydrolase family 19 (chitinase)
At1g05860	47562-48850	Hypothetical protein
At1g05870	51729-50394	Unknown protein
At1g05880	54015-56831	Hypothetical protein
At1g05890	58132-62667	Unknown protein
At1g05900	65397-67538	Expressed protein
At1g05910	69297-75004	Tat-binding protein, putative
At1g05920	75545-76492	Hypothetical protein
At1g05930	77919-79434	Hypothetical protein

Figure A-3.4. Genomic sequence of the *AtCTL1* gene. The sequence length is 1285 bp. It contains three exons and two introns. The three exons are located between 1 to 388, 607 to 766 and 868 to 1285 encoding a protein of 321 amino acids. The bold Gs in the second exon indicate the position of the point mutations of *bim*4-1 at nucleotide 745 and *bim*4-2 at nucleotide 701. The capital letters represent the coding region, with 321 codons. Introns are represented in lowercase.

1	ATGGTGACAATCAGGAGTGGTTCAATCGTGATTTTGGTTCTGCTGGCT
49	GTATCATTTCTGGCCTTGGTTGCCAATGGAGAGGACAAAACGATTAAA
97	GTGAAGAAAGTGAGGGGAAATAAGGTGTGCACGCAAGGATGGGAATGC
145	CAGCTGGTGGTCTAAATACTGCTGTAACCAGACGATATCAGATTACTT
193	TCAGGTTTATCAGTTTGAGCAACTCTTTTCCAAAAGGAACACTCCCAT
241	TGCTCATGCTGTGGTTTCTGGGACTACCAGTCTTTCATTACTGCTGCT
289	GCCCTCTTTGAGCCTCTTGGTTTTGGTACCACTGGAGGAAAGCTCATG
337	GGACAGAAAGAAATGGCTGCCTTTCTCGGTCATGTAGCCAGCAAAACG
385	TCCTgtaagttttccttcattttagtcctctttctacatagttgacca
433	tctaactatgaatagaaaaaaggatgctttaagcttacctccatagct
481	ataccattatattaatctgatcaaactcgacattcagaatcatgaaaa
529	tggatatgccctaagttgcagttggtggtttctatgttgtaagaagct
577	gcatatgagtgttactgtgatgtcttatagGTGGCTATGGAGTTGCAA
625	CAGGAGGGCCTTTAGCTTGGGGTCTGTGCTACAACAGGGAAATGAGCC
673	CAATGCAATCCTACTGTGACGAGTCCTG**G**AAATTCAAGTACCCCTGCA
721	GCCCTGGAGCTGAATACTACGGAC**G**CGGTGCCTTACCCATTTACTGgt
769	acacatttctcttctactttgaagctctagataaaaactgtgtcaaac
817	aatttgcattcgtccatactgaaggtatttttacctgtgtgttatttg
865	aagGAACTTCAACTACGGAGCAGCTGGGGAAGCCCTGAAAGCTGATCT
913	CTTGAACCACCCTGAGTACATTGAGCAAAACGCGACACTTGCATTCCA
961	AGCTGCAATCTGGAGATGGATGACTCCAATCAAGAGAGCTCAGCCCTC
1009	AGCTCACGACATCTTTGTCGGAAACTGGAAACCTACAAAGAACGACAC
1057	TTTGTCCAAGCGTGGCCCGACTTTTGGCAGCACCATGAACGTCCTCTA
1105	CGGAGAGTACACATGTGGTCAAGGTTCCATTGATCCAATGAACAACAT
1153	AATCTCACACTACTTATACTTCCTTGACCTCATGGGTATTGGAAGAGA
1201	AGACGCGGGACCAAACGATGAGCTCAGCTGCGCAGAACAGAAACCTTT
1249	CAACCCTTCAACTGTACCTTCCTCTTCCTCTTCGTAA

Figure A-3.5. Curve analysis for *PRC*, *CTL* and *eIF*4A. The graph shows the crossing points for the three different genes as a function of the logarithm of various cDNA concentrations. Separate linear regression lines have been fitted to each gene date set.

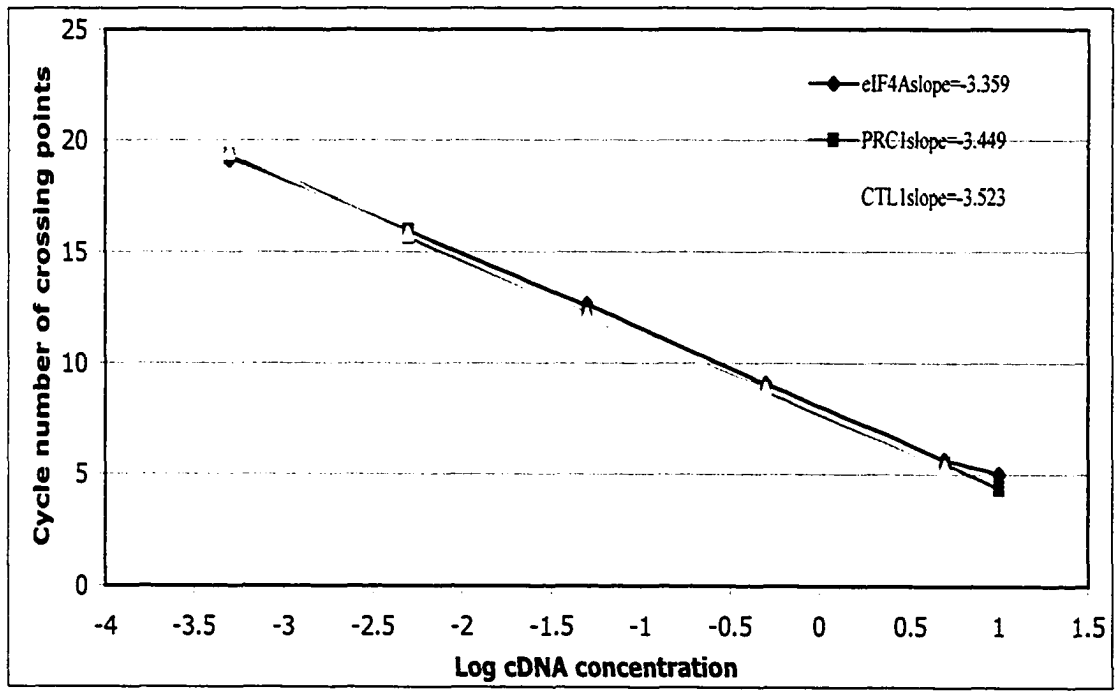

According to an Anova test (Table A-3.6) the slopes do not differ significantly for the three genes. However to show that the mean CP value of the three genes is different, an ANCOVA test, which requires identical slopes was performed. I did an ANCOVA test and the results show that the means of the three curves are indeed different: Fs ~ 5.5 > $F0.05_{[2,13]}$ ~ 3.81 (Table A-3.8). In the above graph I showed that the three genes produce statistically independent CP curves. However, I use each of the three curves independently as a standard curve to estimate Log cDNA from a measured CP.

Figure A-3.6. LightCycler analysis setting report. This report displays fluorescence vs cycle number. SYBR Green I, binds to the minor groove of the DNA double helix and becomes fluorescent. Fluorescence increases with PCR product concentration. Each curve represents an individual sample.

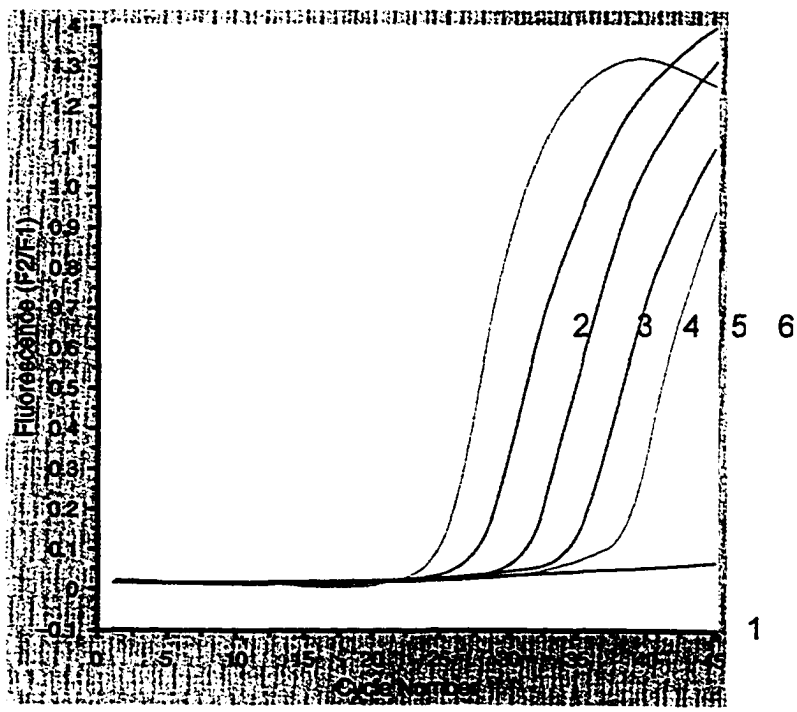

1. No template
2. 3 pg
3. 30 pg
4. 300 pg
5. 3 ng
6. 30 ng

pg and ng of template DNA

Table A-3.2. Statistical summary of transcript levels of *BIM3* (*PRC*) after a 10 hr treatment.

PRC	L10-B	D10-B	L10+B	D10+B	L10-B	L10+B	D10-B	D10+B
mean (mRNA)	417.2	1091.0	636.1	742.9	417.2	636.1	1091.0	742.9
std dev	32.8	38.6	56.6	17.7	32.8	56.6	38.6	17.7
n	4	4	4	4	4	4	4	4
t0.05[dof]	2.4	2.4	2.4	2.4	2.4	2.4	2.4	2.4
ts	26.6		3.6		6.7		16.4	

mRNA concentrations are for light (L) and dark (D) in the absence of BMAA (-B) and for light (L) and dark (D) in the presence of BMAA (+B). The *t*-value (t_s) for all pairs:(L10-B, D10-B), (L10+B; D10+B), (L10-B; L10+B), (D10-B; L10+B) is larger than the critical value of the *t*-distribution at 5% ($t_{0.05[dof]}$). Therefore, we accept the hypothesis that there is a significant difference between the light and dark conditions.

Table A-3.3. Statistical summary of transcript levels of *BIM*4 (*CTL)* after a 10 hr treatment.

CTL	L10-B	D10-B	L10+B	D10+B	L10-B	L10+B	D10-B	D10+B
mean (mRNA)	3143.4	8124.6	4986.4	5188.9	3143.4	4986.4	8124.6	5188.9
std dev	358.2	260.6	231.6	372.6	358.2	231.6	260.6	372.6
n	4	4	4	4	4	4	4	4
t0.05[dof]	2.4	2.4	2.4	2.4	2.4	2.4	2.4	2.4
ts	22.5		0.9		8.6		12.9	

mRNA concentrations are for light (L) and dark (D) in the absence of BMAA (-B) and for light (L) and dark (D) in the presence of BMAA (+B). The *t*-value (t_s) for the (L10-B, D10-B), (L10-B; L10+B) and (D10-B; D10+B) pairs is larger than the critical value of the *t*-distribution at 5% ($t_{0.05[dof]}$). Therefore, we accept the hypothesis that there is a significant difference between the light and dark conditions. But for the pair between light and dark plus BMAA (L10+B; D10+B) t_s is smaller than the critical value of the *t*-distribution indicating that there is no difference between light and dark in the presence of BMAA.

Table A-3.4. Statistical summary of hypocotyl length in absence (MS) and presence (BMAA) of BMAA after 3, 4, 5, 6, and 7 days of dark-grown treatment.

DARK	3 MS	3 BMAA	4 MS	4 BMAA	5 MS	5 BMAA	6 MS	6 BMAA	7 MS	7 BMAA
mean	6.38	5.71	11.61	11.31	14.92	14.84	19.02	16.31	22.42	18.98
std dev	0.78	1.06	1.61	1.48	2.21	1.74	2.43	2.28	1.59	2.27
n	34	34	50	56	39	45	51	52	45	49
variance	0.61	1.12	2.60	2.19	4.86	3.04	5.90	5.20	2.52	5.15
t0.05[*df*]	2.0	2.0	2.0	2.0	2.0	2.0	2.0	2.0	2.0	2.0
t0.001[*df*]	3.5	3.5	3.5	3.5	3.5	3.5	3.5	3.5	3.5	3.5
ts	3.0		1.0		0.2		5.8		8.6	

Under dark conditions the *t*-value of data pairs (t_s) of three, four, and five days of treatment are smaller than the critical value of the *t*-distribution at 5% ($t_{0.05[dof]}$). We cannot reject the hypothesis that there is no significant difference in the hypocotyl lengths between BMAA treated and non BMAA-treated samples. However, at day six and seven we find a very significant difference between BMAA treated and non BMAA-treated samples at the <0.1% confidence level.

Table A-3.5. Statistical summary of hypocotyl length in absence (MS) and presence (BMAA) of BMAA after 3, 4, 5, 6, and 7 days of light-grown treatment.

LIGHT	3 MS	3 BMAA	4 MS	4 BMAA	5 MS	5 BMAA	6 MS	6 BMAA	7 MS	7 BMAA
mean	1.742	2.222	2.061	3.383	2.037	4.027	2.045	5.600	2.746	7.630
std dev	0.259	0.447	0.295	0.495	0.328	0.756	0.203	0.803	0.464	0.825
n	45	45	44	46	49	51	51	49	52	53
variance	0.07	0.20	0.09	0.25	0.11	0.57	0.04	0.64	0.22	0.68
t0.05[*df*]	2.0	2.0	2.0	2.0	2.0	2.0	2.0	2.0	2.0	2.0
t0.001[*df*]	3.5	3.5	3.5	3.5	3.5	3.5	3.5	3.5	3.5	3.5
ts	6.2		15.5		17.2		30.1		37.5	

Under light condition, since the *t*-value of each data pair (t_s) is larger than the critical value of the *t*-distribution for any pair, one concludes that the mean etiolated hypocotyl lengths in BMAA treated and non BMAA-treated samples are significantly different for all pairs.

Table A-3.6. Preliminary Anova of the dependent variable.

Source of variation	*df*	SS	MS	Fs
Groups	2	5.203	2.601	0.079
Within	14	458.928	32.781	
Total	16	464.131		

The test is unable to detect differences among the means from the three genes. The groups do not differ significantly. $F_{0.05[2, 30]} = 3.32$.

Table A-3.7. Significance test of slope variation.

$SS_{among\ b's}$=	$\sum d^2_{YY\ (within)} - \sum_a \sum_n d^2_{YX}$	0.1623
$MS_{among\ b's}$=	$SS_{among\ b's}$ / a - 1	0.0811
F_s =	$MS_{among\ b's}$ / $\langle S \rangle^2_{Y.X}$	5.6196

In an analysis of covariance the assumption is that separate regression slopes of the groups do not differ but represent a single slope. If the slopes were identical $SS_{among\ b's}$ would be zero and Fs would be smaller than $F_{0.05[2,11]} = 3.98$. However, the calculation results in a larger value for Fs and I conclude that there is no significant evidence for identical slopes of the three curves. The null hypothesis states that the separate regressions of crossing points on log concentration for each group do not differ in slope. $F_{0.05[2,11]} = 3.98$, $F_{0.01[2,11]} = 7.21$, $F_{0.001[2,11]} = 13.08$. It is accepted at 1% and 0.1%

Table A-3.8. Final ANCOVA table.

Source of variation	*df*	SS	MS	F_s
Adjusted means	2	0.271	0.136	5.493
Error	13	0.321	0.025	

Testing the null hypothesis for ANCOVA. It states that there are no differences among sampled means and all three regression lines coincide. $F_{0.05[2,13]} = 3.81$, $F_{0.02[2,13]} = 5.49$. Therefore we conclude with a probability of less than 5% (approximately 2%) that there is not a significant probability that the means of the three slopes are equal.

Chapter 4

BMAA May Alter Ion Sensitivity in *Arabidopsis* Seedlings

ABSTRACT

Mammalian ionotropic glutamate receptors function to perceive glutamate during neurotransmission. Binding of glutamate to the ligand-binding domain of the glutamate receptors results in the gating of the transmembrane pore, allowing Na^+ inward and K^+ outward. In an attempt to understand the activity of these ions on plant GLRs, I cultivated *Arabidopsis* seedlings in K^+Cl^- and Na^+Cl^- at increasing concentrations (120, 140, 160mM). Additionally I looked at the physiological effect these ions have in the presence of BMAA. High concentrations of Na^+ or K^+ have opposite effects on the survival of the Arabidopsis seedlings. At high concentrations of Na^+, seedling survival is not affected; however, when BMAA-treated seedlings are exposed to high concentrations of Na^+, seedling survival is inhibited. In contrast, seedlings are hypersensitive to high concentrations of K^+, inducing seedling death. Surprisingly, BMAA-treated seedlings survive when grown in high concentrations of K^+. A model suggesting the mode of action of BMAA on regulating the internal ion concentration in plant cells is proposed. These results suggest that BMAA may mediate ion sensitivity in *Arabidopsis*.

INTRODUCTION

Characterization of plant *GLRs*

Based on sequence homology, twenty genes coding for iGLRs in plants have been recently identified and classified into three different branches (Lacombe et al, 2001b). Numerous efforts to understand the molecular mechanisms and to functionally characterize the *AtGLRs* are in progress. Characterization of three *GLR* genes has yielded preliminary data that indicates *AtGLRs* are mediators of Ca^{2+} ions. Plants over-expressing the *AtGLR*3.2 gene showed symptoms of Ca^{2+} deficiency and hypersensitivity to K^+ and Na^+ stress (Kim et al., 2001). The Ca^{2+} level in transgenic overexpressors and wild-type plants did not differ significantly, but the Ca^{2+} deficiency symptoms in overexpressors were alleviated with additional Ca^{2+}. This suggests that Ca^{2+} usage rather than Ca^{2+} uptake was affected in these plants. The hypersensitivity to K^+ and Na^+ ionic stress in the transgenic plants was also alleviated by the addition of Ca^{2+}, indicating that the plants are deficient in Ca^{2+}.

Characterization of *AtGLR*3.7 (Cheffings, 2001) and *AtGLR*3.4 (Lacombe et al., 2001a) has also been attempted. These two iGLRs were expressed in oocytes and the results showed the involvement of Ca^{2+} without the participation of Glu or an iGluR agonist. *AtGLR*3.7 was proposed to be an active Ca^{2+} permeable non-selective cation channel (Cheffings, 2001) and *AtGLR*3.4 a mediator of Ca^{2+} influx (Lacombe et al., 2001a). Despite the numerous efforts to continue characterizing the function of AtGLRs, the progress is slow, as it is often difficult to replicate the results obtained in electrophysiological studies or to obtain phenotypes by deactivating gene function. In

the latter case, this may be due to redundant function of the twenty GLR genes present in *Arabidopsis*.

Ca^{2+} signaling in plants

In plants, cytosolic calcium fluctuations are speculated to be involved in transducing environmental signals into plant responses. Changes in cellular metabolism, such as cell turgor and nutrient uptake are the result of ion channel activation. Such metabolic regulation can be direct, as in the case of some ion channels that are permeable to and activated by Ca^{2+} ions (Bewell et al., 1999), or indirect by the activation of downstream components; for example, by affecting calcium-activated calmodulin (Ca^{2+}/CaM) (Hong et al., 1999, Harper et al., 1998).

In plants, Ca^{2+} channel activity has been reported to mediate depolarization and hyperpolarization of the plasma membrane (Gelli et al, 1997a,b). Furthermore, glutamate receptors, by forming active ion channels, are suggested to participate in the mediation of Ca^{2+} fluctuations through the plasma membrane (Davenport, 2002; Sanders et al., 2002). To understand the mechanisms involved in AtGLRs functioning in plants, Kim et al. (2001) created a transgenic *Arabidopsis* line overexpressing an *AtGLR*. Overexpression of AtGLR causes the plants to be hypersensitive to Na^+ and K^+ stress. High external concentrations of Na^+ and K^+ in plant cultures have been associated with reduced absorption of Ca^{2+} inducing Ca^{2+} deficiency in plants (Robson and Pitman, 1983), Kim et al. (2001) concluded that it is the overexpression of the *GLR* that directly disturbed the Ca^{2+} transport. To explore the link between Na^+ and K^+ ions and GLR genes, I investigated the effect of high concentrations of Na^+ and K^+ on

Arabidopsis seedlings. Additionally I looked at ion-treated plants in the presence of S(+)-β-methyl-α, β-diaminopropionic acid (BMAA) because it has been postulated that BMAA is involved in blocking plant GLR signaling in *Arabidopsis* (Brenner et al., 2000). In this chapter, I report the effects caused by high concentrations of Na^+ or K^+ ions on *Arabidopsis* seedlings and the effect caused by BMAA on ion-treated plants.

RESULTS

BMAA-treated *Arabidopsis* seedlings respond differently to Na^+ and K^+ ions

To determine the effect that high concentrations of Na^+ and K^+ ions have on BMAA-treated *Arabidopsis* seedlings, *Arabidopsis* plants were grown in medium containing increasing concentrations of NaCl or KCl (80, 100, 120, 140mM) in the absence or presence of 60μM BMAA. The hypocotyl length of 7 day-old seedlings was quantified for all treatments (Fig. 4.1). In the absence of BMAA, 80mM NaCl appears to have no effect in hypocotyl elongation when compared to untreated seedlings but an increase in NaCl concentration leads to a significant decrease in hypocotyl length. In 80mM KCl there is a 30% increase in hypocotyl length when compared to untreated seedling and - similarly to NaCl - higher concentrations decrease the hypocotyl elongation when compared with untreated seedlings. In the presence of BMAA, induction of hypocotyl elongation on seedlings grown in media at concentrations of 80 and 100mM NaCl is 60% to 80%, while in KCl BMAA induces a 50% to 70% induction in concentrations of 80, 100 and 120mM. The addition of BMAA to medium at 120 and 140mM concentrations of NaCl has no effect on elongation, but does cause detrimental effects

to the seedling survival (Fig. 4.2). In contrast, at concentrations of 140mM KCl, BMAA does no affect seedling growth, when compared to BMAA-untreated seedlings (Fig. 4.3).

In order to determine the effect of BMAA in *Arabidopsis* seedlings at concentrations higher than 140mM of NaCl and KCl, *Arabidopsis* seedlings were grown for 14 d on medium containing increasing amounts of NaCl or KCl (120, 140 and 160mM) in the presence and absence of 60μM BMAA. As shown in Figure 4.4, high concentrations of NaCl suppress seedling development but the plants remain alive. In contrast, supplementing the medium with BMAA becomes lethal to seedling survival. The opposite effect is shown in KCl (Fig. 4.5); at high concentrations of KCl, seedling survival is inhibited. On this KCl containing medium, wild-type plants are dead, but supplementing the medium with BMAA reverses the effect and BMAA rescues the seedling (Figure 4.5). Figure 4.6 compares *Arabidopsis* seedlings grown in 160mM NaCl or KCl in the absence and the presence of BMAA.

DISCUSSION

Conclusive results cannot be derived from these experiments because several factors seem to play a role in the outcome of the experiment. When the experiments were repeated, the results were not consistent. However, some of the observed effects can be interpreted by considering electrophysiological aspects in cells, by assuming high external concentrations of Na^+ or K^+ do not kill the cell unless there is ion influx inversing the membrane potential, and that BMAA persistently activates ionotropic

channels similar to the effect that high concentrations of glutamate have on mammalian ionotropic glutamate receptors (Hartley, 1993).

In the animal nervous system, K^+ is actively concentrated inside the cell and Na^+ is actively extruded to the extracellular space. At rest, cells have an excess of positive charges on the outside and negative charges inside; whenever an action potential is generated, two Na^+ ions enter the cell and one of K^+ leaves the cell. Normally, Na^+ entering from the outside of a cell causes depolarization (reduction of the charge separation) and, consequently, more Na^+ channels open. From the observation that the addition of BMAA is lethal to seedlings grown in high concentrations of Na^+, whereas BMAA-nontreated seedlings survive, I conclude: GLRs are inactive in the absence of the ligand, however when BMAA - acting as a ligand - is present the effect is reversed. Because BMAA keeps the channels open, excess Na^+ can enter the cell along its gradient and eventually kill the cell (Fig. 4.7A).

Under normal conditions, in the presence of Glu, and after depolarization by Na^+, K^+ channels open and the steady efflux of K^+ induces repolarization of the membrane. The observation that BMAA-treated *Arabidopsis* seedlings survive high concentrations of K^+ but non-treated samples died can be interpreted as follows: Assuming that in the absence of the ligand the iGluR channels remained closed, K^+ ions cannot leave the cell in order to properly maintain the membrane potential. Additionally the external high concentration of K^+ impairs the ability of other potassium channels to allow K^+ efflux. Under these conditions, an excess of K+ ions accumulates inside the cell, becoming increasingly lethal and ultimately killing the cell. In contrast, in the presence of high extracellular K^+ and BMAA, BMAA activates the receptor and keeps

the channel open. Now, K^+ can be transported through the persistently activated iGluR channels against the gradient, thus maintaining the membrane potential and preventing the seedling from dying.

Ion channels in the cyanobacteria Synechocystis (GluR0) (Chen et al., 1999) bind glutamate but form potassium-selective channels. Additionally, GluR0 responses in the presence of K^+ are stopped when K^+ is replaced by Na^+. These GluR0 receptors show the strongest sequence similarity to *Arabidopsis* Glu receptors. My experiments suggest that AtGLRs are permeable to both K^+ and Na^+. It is possibile that one subset of AtGLR could function in a similar manner as GluR0 in specifically mediating K^+ ions by binding BMAA, while a different subset of AtGLR could mediate Na^+ ions.

The detailed mechanisms and actions of BMAA in these experiments remain unclear. The great diversity of K^+ channels and transporters in *Arabidopsis* at the whole-plant level (Véry et al., 2003) may play a more fundamental role. Further detailed investigations are needed to understand the surprising outcome of these experiments.

MATERIALS AND METHODS

Plant Growth Conditions

After surface-sterilization, *Arabidopsis* seed (Lehle Seeds, Round Rock, TX) was plated on Murashige and Skoog (Sigma) medium, pH 5.7, supplemented with 1% sucrose, and 8% agar. After sterilization of the medium and cooling to 50°C, 60μM

BMAA (Sigma G-1501) plus different concentrations of Na^+Cl^- or K^+Cl^- were added from sterile stocks. Seed was pretreated for 3 days at 4°C, before grown vertically in square plates (100 x 15mm) for 7 or 14 days.

Figure 4.1 Quantification of light-grown hypocotyls in NaCl or KCl in the absence and presence of BMAA. Arabidopsis plants were grown on increasing concentrations of NaCl or KCl (80,100, 120,140mM) in the absence and presence of BMAA (60μM) for 7 d. The average hypocotyl length for each treatment is shown. Error bars show the SD of the mean. NT= no treatment.

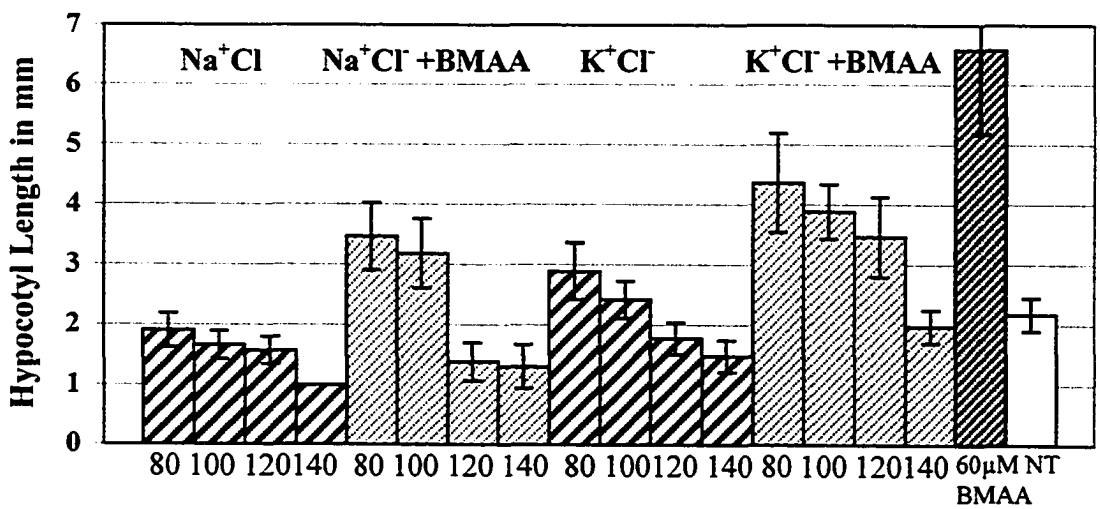

Figure 4-2. Effect of BMAA on one week-old *Arabidopsis* seedlings grown on increasing concentrations of NaCl. Seedlings were grown for 7 days in increasing concentrations of NaCl (80, 100, 120, 140mM) in the absence and presence of BMAA. At high concentrations of NaCl, BMAA inhibits seedlings growth.

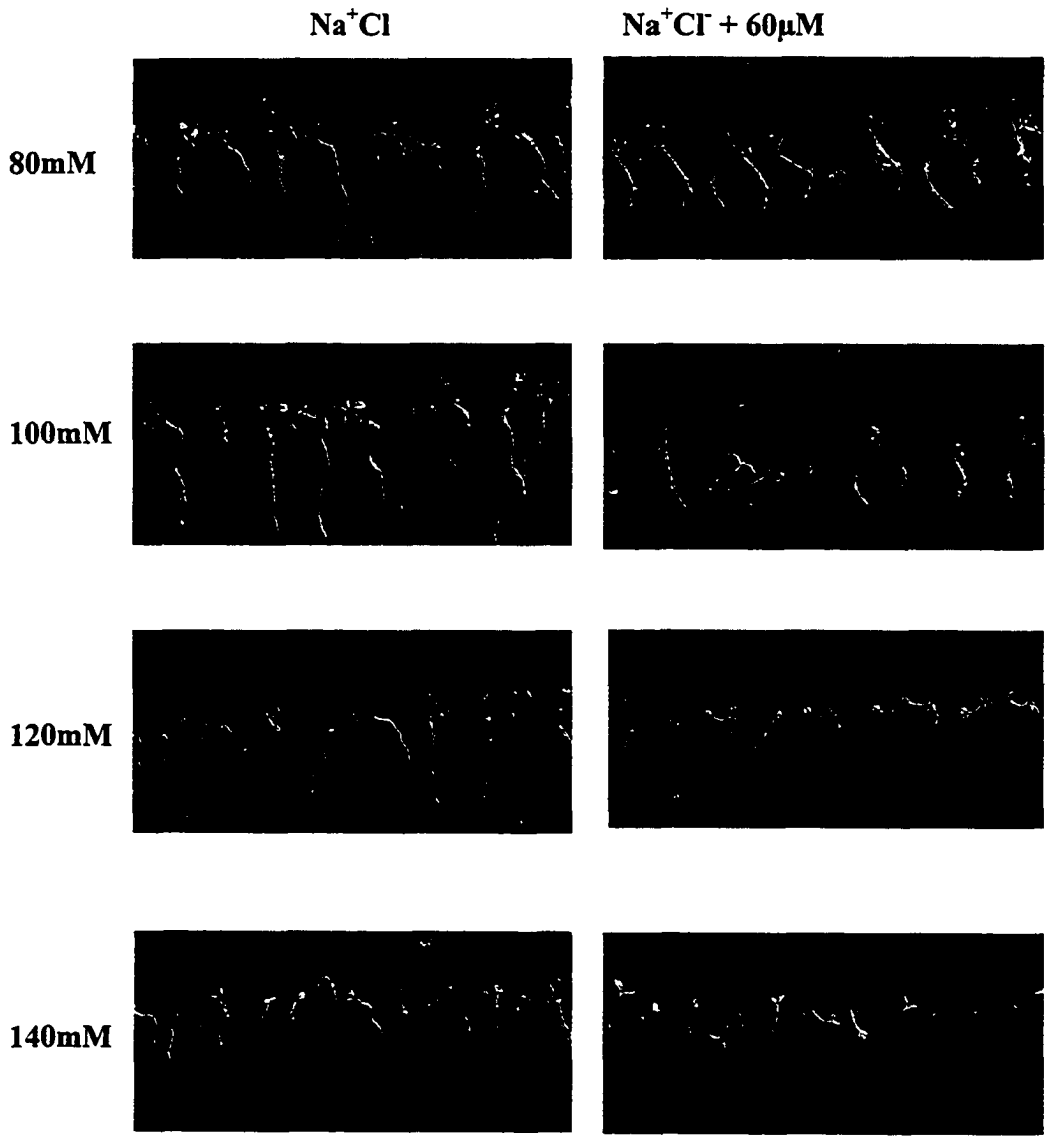

Figure 4-3. Effect of BMAA on one week-old *Arabidopsis* seedlings grown on increasing concentrations of KCl. Seedlings were grown for 7 days in increasing concentrations of KCl (80, 100, 120, 140mM) in the absence and presence of BMAA. At high concentrations of KCl, BMAA appears to have no effect, when compared with untreated plants.

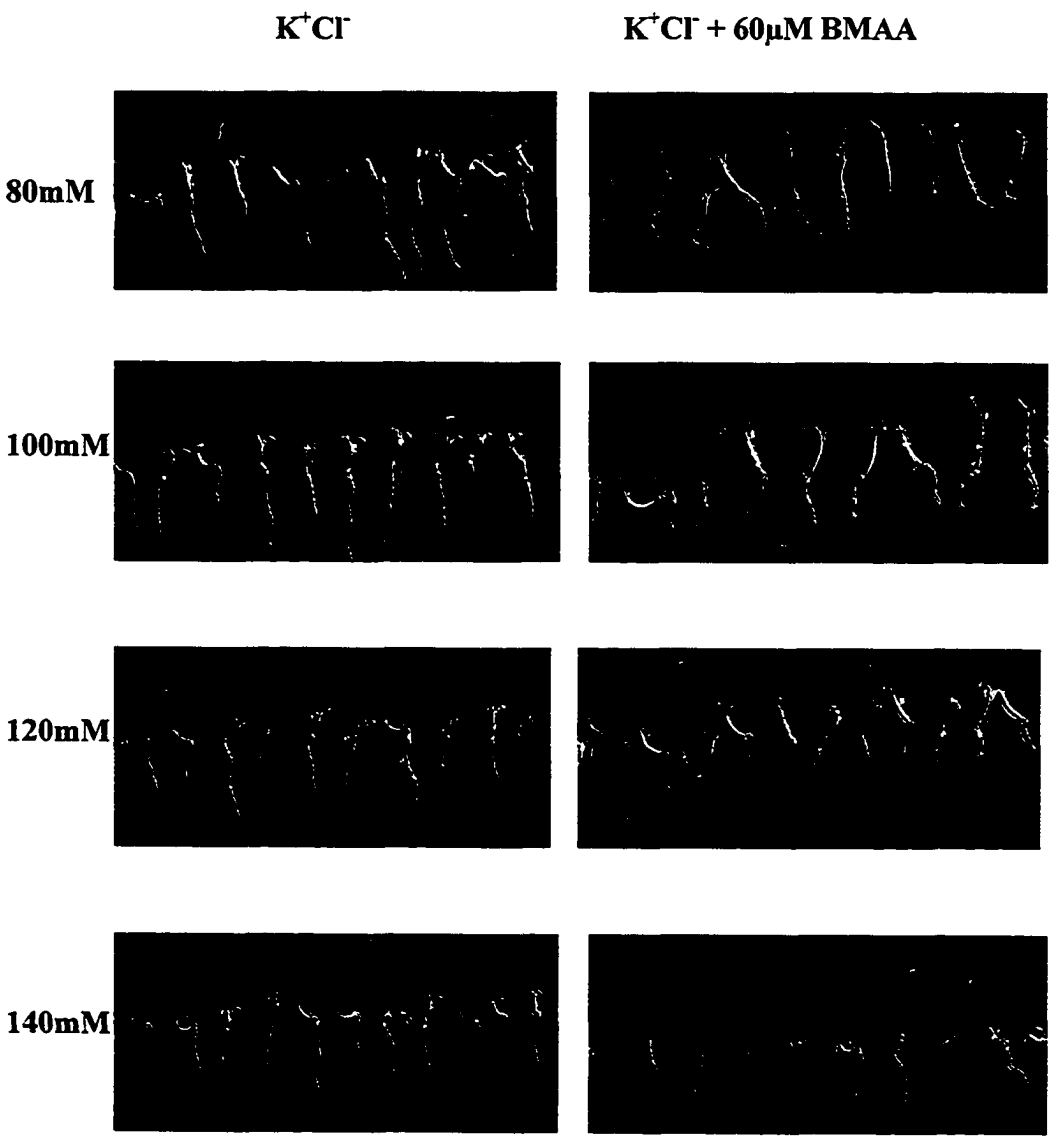

Figure 4.4. Effect of BMAA in two week-old light-grown *Arabidopsis* seedlings on high concentrations of NaCl. Seedlings were grown for 14d in increasing concentrations of NaCl (120, 140, 160mM). BMAA starts inhibiting seedling growth at concentrations of 140 mM NaCl.

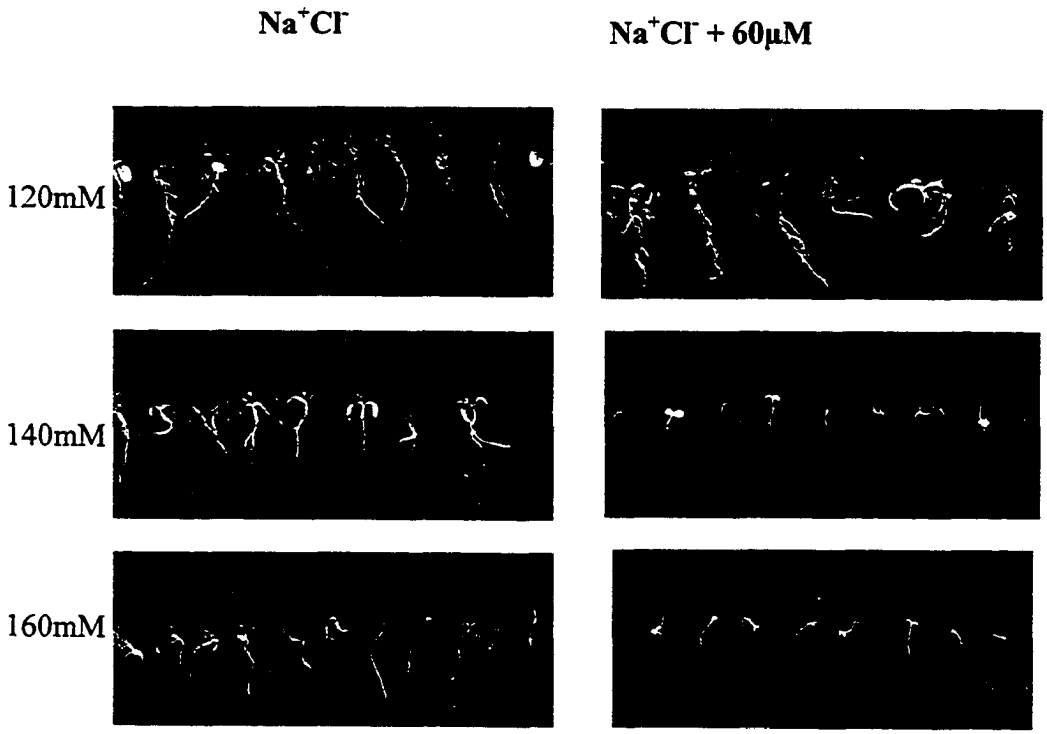

Figure 4.5. Effect of BMAA in two week-old light-grown *Arabidopsis* seedlings on high concentrations of KCl. Seedlings were grown for 14d in increasing concentrations of KCl (120, 140, 160mM). High concentrations of KCl inhibit seedling growth, but BMAA rescues the seedlings from these detrimental effects.

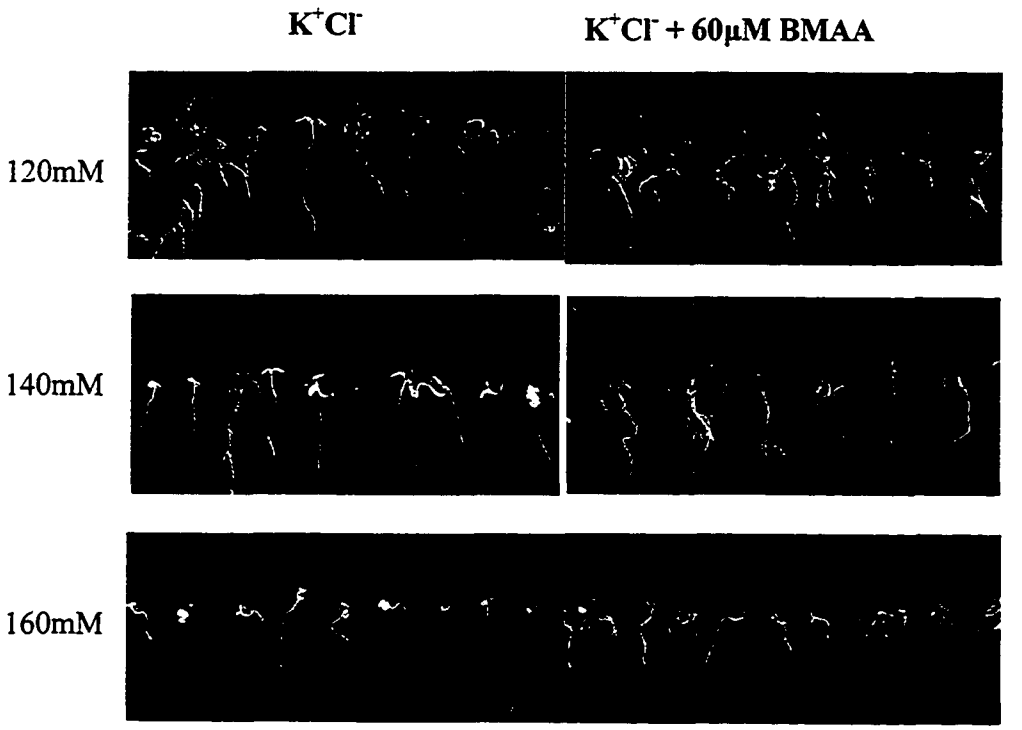

Figure 4.6. Comparison of the effect of BMAA on two week-old *Arabidopsis* seedlings grown on high concentrations of NaCl or KCl. Seedlings were grown for 14d in MS medium at concentrations of 160mM NaCl or KCl in the presence and absence of BMAA.

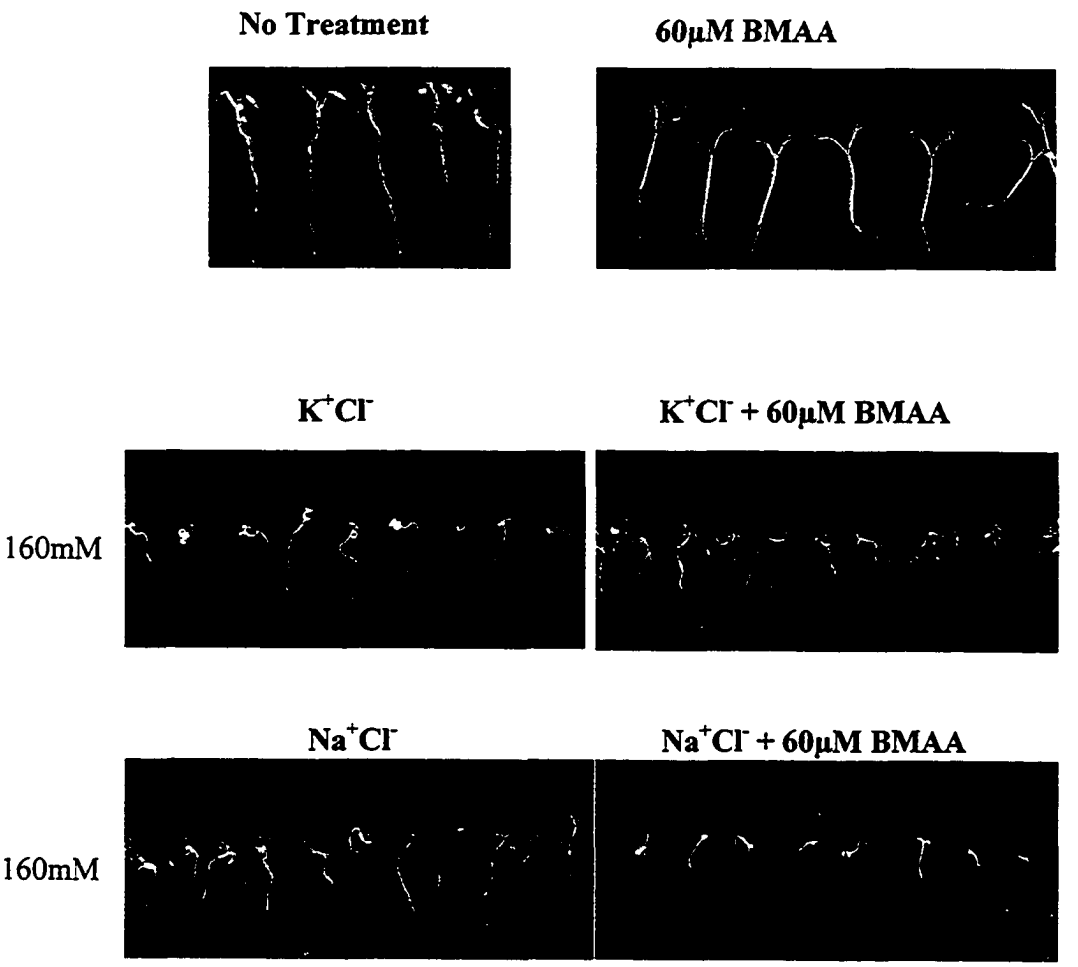

Figure 4.7. The opposite effect of Na^+ and K^+ on *Arabidopsis* seedlings is reversed by BMAA.

(A) On the plasma membrane, in the absence of the ligand and external high concentrations of Na^+, the GLR channels remain close. In the presence of BMAA, the activation of the receptors is persistent, and Na^+ moves in and kills the cell.

(B) Normally the GLRs are close and at high external concentration of K^+ the plant dies, since K^+ can not maintain the membrane potential by flowing out, but in the presence of BMAA the GLRs open and K^+ efflux, rescues the seedling from dying.

A

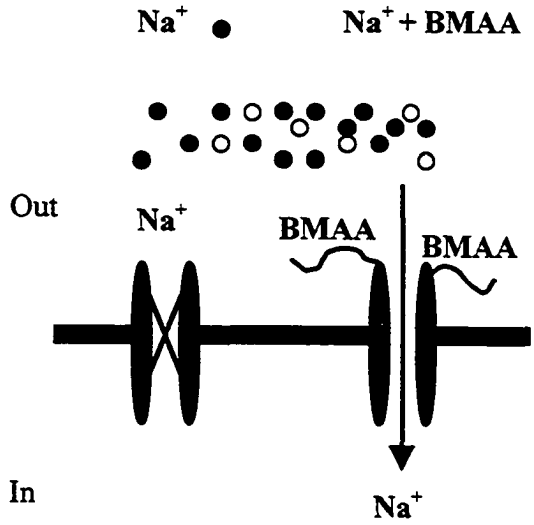

Rescues Seedling Kills Seedling

B

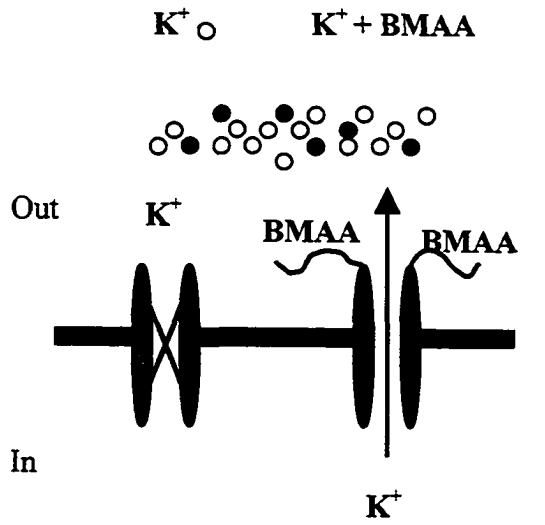

Kills Seedling Rescues Seedling

REFERENCES

Abeles, F.B., Morgan, P.W., Saltveit, M.E., Jr. (1992). Ethylene in plant biology (Academic, New York), 2nd Ed.

Asztely, F., Gustafsson, B. (1996). Ionotropic glutamate receptors: Their role in the expression of hippocampal synaptic plasticity. Mol. Neurobiol. **12**, 1-11.

Banack, S.A., Cox, P.A. (2003). Biomagnification of cycad neurotoxins in flying foxes – Implications for ALS-PDC in Guam. Neurology **61**, 387-389.

Bell, C.J., Ecker, J.R. (1994). Assignment of 30 microsatellite loci to the linkage map of *Arabidopsis*. Genomics **19**, 137-144.

Bewell, M.A., Maathius, F.J., Allen, G.J., Sander, D. (1999). Calcium-induced calcium release mediated by a voltage-activated cation channel in vacuolar vesicles from red beet. FEBS Letter **458**, 41-44.

Brenner, E.D., Martinez-Barboza, N., Clark, A.P., Liang, Q.S., Stevenson, D.W., Coruzzi, G.M. (2000). *Arabidopsis* mutants resistant to S(+)-β-methyl-α, β-diaminopropionic acid. A cycad-derived glutamate receptor agonist. Plant Physiol. **124**, 1615-1624.

Brownson, D.M. (1996). A Study of known excitotoxic compounds and isolated nonprotein amino acids from cycads. Dissertation presented to The University of Texas at Austin.

Chang, C., Meyerowitz, E.M. (1995). The ethylene hormone response in *Arabidopsis*: a eukaryotic two-component signaling system. Proc. Natl. Acad. Sci. USA **92**, 4129-4133.

Charlton, T.S., Marini, A.M., Markey, S.P., Norstog, K., Duncan, M.W. (1992). Quantification of the neurotoxin 2-amino-3-(Methylamino)-Propanoic acid (BMAA) in Cycadales. Phytochem. **31**, 3429-3432.

Cheffings, C.M. (2001). Calcium channel activity of a plant glutamate receptor homologue. 12th International Workshop on Plant Membrane Biology. Madison, WI.

Chen, G-Q., Cui, C., Mayer, M.L., Gouaux, E. (1999). Functional characterization of a potassium-selective prokaryotic glutamate receptor. Nature **402**, 817-821.

Chiu, J., DeSalle, R., Lam, H., Meisel, L., Coruzzi, G. (1999). Molecular evolution of putative plant glutamate receptors and their relationship to animal ionotropic glutamate receptors. Mol. Biol. Evol. **16**, 826-838.

Cho, M.H., Spalding, E.P. (1996). An anion channel in *Arabidopsis* hypocotyls activated by blue light. Proc. Natl. Acad. Sci. USA **93**, 8134-8138.

Choi, D.W. (1988). Calcium-mediated neurotoxicity: relationship to specific channel types and role in ischemic damage. Trends Neurosci. **11**, 465-469.

Chory, J., Aguilar, N., Peto, C.A. (1991). The phenotype of *Arabidopsis thaliana det*1 mutants suggests a role for cytokinins in greening. Sympo. Soc. Exp. Biol. **41**, 21-29.

Chory, J., Peto, C.A., Feinbaum, R., Pratt, L., Ausubel, F. (1989). *Arabidopsis thaliana* mutant that develops as a light grown plant in the absence of light. Cell **58**, 991-999.

Cox, P.A., Sacks, O.W. (2002). Cycad neurotoxins, consumption of flying foxes, and ALS-PDC disease in Guam. Neurology **58**, 956-959

Davenport, R. (2002). Glutamate receptors in plants. Ann. Bot. **90**, 549-557.

Deng, X-W., Caspar, T., Quail, P.H. (1991). *cop*1: a regulatory locus involved in light-controlled development and gene expression in *Arabidopsis*. Genes & Develop. **5**, 1172-1182.

Dennison, K.I., Spalding, E.P. (2000). Glutamate-gated calcium fluxes in *Arabidopsis*. Plant Physiol. **124**, 1511-14.

Desnos, T., Orbovic, V., Bellini, C., Kronenberger, J., Caboche, M., Traas, J., Höfte, H. (1996). *Procuste*1 mutants identify two distinct genetic pathways controlling hypocotyl cell elongation, respectively in dark- and light-grown *Arabidopsis* seedlings. Development **122**, 683-693.

Dingledine, R., Borges, K., Bowie, D., Traynelis, S.F. (1999). The glutamate receptor ion channels. P. Pharmacol. Rev. **51**, 7-61.

Dixon, R.A., Harrison, M.J., Lamb, D.J. (1994). Early events in the activation of plant defense responses. Annu. Rev. Phytopathol. **32**, 479-501.

Dubos, C., Huggins, D., Grant, G.H., Knight, M.R., Campbell, M.M. (2003). A role for glycine in the gating of plant NMDA-like receptors. Plant J. **35**, 800-810.

Duncan, M.W., Kopin, I.J., Crowley, J.S., Jones, S.M., Markey, S.P. (1989). Quantification of the putative neurotoxin 2-amino-3-(methylamino) propanoic acid (BMAA) in Cycadales: Analysis of the seeds of some members of the family Cycadaceae. J. Analytical Toxic. **13**, 169-176.

Duncan M.W., Steele, J.C., Kopin, I.J., Markey, S.P. (1990) 2-amino-3-(methylamino)-propanoic acid (BMAA) in cycad flour: an unlikely cause of amyotrophic lateral sclerosis and parkinsonism-dementia of Guam. Neurology **40**, 767-772.

Ebel, J., Scheel, D. (1992). Elicitor recognition and signal transduction, in Genes involved in plant defense, eds. Boller, T. and Meins, F. (Springer, Vienna). 183-205.

Edwards, K., Johnstone, C., Thompson, C. (1991). A simple and rapid method for the preparation of plant genomic DNA for PCR analysis. Nucleic Acids Res. **19**, 1349.

Ellis, C., Karafyllidis, I., Wasternack, C., Turner, J.G. (2002). The *Arabidopsis* mutant *cev1* links cell wall signaling to jasmonate and ethylene responses. Plant Cell **14**, 1557-1566.

Evans, M.L. (1985). The action of auxin on plant cell elongation. Crit. Rev. Plant Sci. **2**, 317-365.

Fagard, M., Desnos, T., Desprez, T., Goubet, F., Refregier, G. M., McCann, M., Rayon, C., Vernhettes, S., Höfte, H. (2000). *PROCUSTE1* Encodes a cellulose synthase required for normal cell elongation specifically in roots and dark-grown hypocotyls of *Arabidopsis*. Plant Cell **12**, 2409-2423.

Favaron, M., Manev, H., Siman, R., Bertolino, M., Szekely, A.M., DeErausquin, G., Guidotti, A., Costa, E. (1990). Down-regulation of protein kinase C protects cerebellar granule neurons in primary culture from glutamate-induced neuronal death. Proc. Nat. Acad. Sci. USA **87**, 1983-1987.

Gasic, G.P., Hollmann, M. (1992). Molecular neurobiology of glutamate receptors. Annu. Rev. Physiol. **54**, 507-536.

Gelli, A., Blumwald, E. (1997a). Hyperpolarization-activated Ca^{2+}-permeable channels in the plasma membrane of tomato cells. J. Membr. Biol. **155**, 35-45.

Gelli, A., Higgins, V.J., Blumwald, E. (1997b). Activation of plant plasma membrane Ca^{2+}-permeable channels by race-specific fungal elicitors. Plant Physiol. **113**, 269-279.

Harper, J.F., Hong, B., Hwang, I., Qing Guo, H., Stoddard, R., Huang, J.F., Palmgren, M., Sze, H. (1998). A novel calmodulin-regulated Ca^{2+}-ATPase (*ACA2*) from *Arabidopsis* with an N-terminal autoinhibitory domain. J. Biol. Chem. **273**, 1099-1106.

Hartley, D.M., Kurth, M.C., Bjerkness, L, Weiss, J.H., Choi, D.W. (1993). Glutamate receptor-induced 45Ca2+ accumulation in cortical cell culture correlates with subsequent neuronal degeneration. J. Neurosci. **13**, 1993-2000.

Hollmann, M, Heinemann, S. (1994). Cloned glutamate receptors. Annu Rev Neurosci. **17**, 31-108.

Hong, B., Ichida, A., Wang, Y., Gens, J.S., Pickard, B.G., Harper, J.F. (1999). Identification of a calmodulin-regulated Ca^{2+}-ATPase in the endoplasmic reticulum. Plant Physiol. **119**, 1165-1176.

Jacobsen, S.E., Olszewski, N.E. (1993). Mutations at the *SPINDLY* locus of *Arabidopsis* alter gibberellin signal transduction. Plant Cell **5**, 887-896.

Johnson, J.W., Ascher, P. (1987). Glycine potentiates the NMDA response in cultured mouse brain neurons. Nature **325**, 529-531.

Kang, J., Turano, F.J. (2003). The putative glutamate receptor 1.1 (*AtGLR*1.1) functions as a regulator of carbon and nitrogen metabolism in *Arabidopsis thaliana*. Proc. Natl. Acad. Sci. USA **100**, 6872-6877.

Khabazian, I., Bains, J.S., Williams, D.E., Cheung, J., Wilson, J.M.B., Pasqualotto, B.A., Pelech, S.L., Andersen, R.J., Wang, Y.T., Liu, L., Nagai, A., Kim, S.U., Craig, U-K., Shaw, C.A. (2002). Isolation of various forms of sterol β-D-glucoside from the seed of *Cycas circinalis*: neurotoxicity and implications for ALS-parkinsonism dementia complex. J. Neurochem. **82**, 516-528.

Kim, S.A., Kwak, J.M., Jae, S.-K., Wang, M-H, Nam, H.G. (2001). Overexpression of the *AtGluR*2 gene encoding an *Arabidopsis* homolog of mammalian glutamate receptor impairs calcium utilization and sensitivity to ionic stress in transgenic plants. Plant Cell Physiol. **42**, 74-84.

Kinnersley, A.M., Turano, F.J. (2000). Gamma aminobutyric acid (GABA) and plant responses to stress. Crit. Rev. Plant Sci. **19**, 479-509.

Kleckner, N.W., Dingledine, R. (1988). Requirement for glycine in activation of NMDA receptors expressed in *Xenopus* oocytes. Science **241**, 835-837.

Knight, M.R., Campbell, A.K., Smith, S.M., Trewavas, A.J. (1991). Transgenic plant aequorin reports the effects of touch and cold-shock and elicitors on cytoplasmic calcium. Nature **352**, 524-526

Knight, M.R., Smith, S.M., Trewavas, A.J. (1992). Wind induced plant motion immediately increases cytosolic calcium. Proc. Natl. Acad. Sci. USA **89**, 4967-71.

Konieczny, A., Ausubel, F.M. (1993). Procedure for mapping *Arabidopsis* mutations using co-dominant ecotype-specific PCR-based marker. Plant J. **4**, 403-410.

Lacombe, B., Meyerhoff, O., Steinmeyer, R., Becker, D., Hedrich, R. (2001a). Role of *Arabidopsis* ionotropic glutamate receptors. Abstract. Association "Canaux Ioniques" 12eme Colloque, La Londe les Maures.

Lacombe, B., Becker, D., Hedrich, R., DeSalle, R., Hollman, M., Kwak, J.M., Schroeder, J.I., Le Novère, N., Nam, H.G., Spalding, E.P, Tester, M., Turano, F.J., Chiu, J., Coruzzi, G. (2001b). The identity of plant glutamate receptors. Science **292**, 1486-1487.

Lam, H.M., Chiu, J., Hsieh, M.H., Meisel , L., Oliveira, I.C., Shin, M., Coruzzi , G. (1998a). Glutamate-receptor genes in plants. Nature **396**, 125-126.

Lam, H.M., Hsieh, M.H., Coruzzi, G. (1998b). Reciprocal regulation of distinct asparagine synthetase genes by light and metabolites in *Arabidopsis thaliana*. Plant J. **16**, 345-353.

Lewis, B.D., Karlin-Neumann, G., Davis, R.W., Spalding, E.P. (1997). Ca(2+)-activated anion channels and membrane depolarizations induced by blue light and cold in *Arabidopsis* seedlings. Plant Physiol. **114**, 1327:1334.

Lobner, D., Lipton, P. (1993). Intracellular calcium levels and calcium fluxes in the CA1 region of the rat hippocampal slice during in vitro ischemia: relationship to electrophysiological cell damage. J. Neurosci. **13**, 4861-4871.

MacDermott, A.B., Dale, N. (1987). Receptors, ion channels and synaptic potentials underlying the integrative actions of excitatory amino acids. Trends Neurosci. **10**, 280-284.

Maren, S., Baudry, M. (1995). Properties and mechanisms of long-term synaptic plasticity in the mammalian brain: relationships to learing and memory. Neurobiol. Learn Mem. **63**, 1-18.

Masucci, J.D., Schiefelbein, J. (1996). Hormones act downstream of *TTG* and *GL2* to promote root hair outgrowth during epidermis development in the *Arabidopsis* root. Plant Cell **8**, 1505-1517.

Mayer, M.L., Partin, K.M., Patneau, D.K., Wong, L.A., Vyklicky, L. Jr., Benveniste, M.J., Bowie, D. (1995). Desensitization at AMPA, kainate and NMDA receptors, in Excitatory Amino Acids and Synaptic Function (WhealH and Thomson A eds) 2nd ed., pp 89-98, Academic Press, New York.

Miséra, S., Müller, A.J., Weiland-Heidecker, U., Jürgens, G. (1994). The *FUSCA* genes of *Arabidopsis*: negative regulators of light responses. Mol. Gene Genetics **244**, 242-252.

Nakanishi, S. (1992). Molecular diversity of glutamate receptors and implications for brain-function. Science, **258**, 597-603.

Nichols, R.A., Sihra, T.S., Czernik, A.J., Nairn, A.C., Greengard, P. (1990). Calcium/calmodulin-dependent protein kinase II increases glutamate and noradrenaline release from synaptosomes. Nature **343**, 647-651.

Oliveira, I.C., Coruzzi, G., (1999). Carbon and amino acids reciprocally modulate the expression of glutamine synthetase in *Arabidopsis*. Plant Physiol. **221**, 301-309.

Poovaiah, B.W., Leopold, A.C. (1973a). Inhibition of abscission by calcium. Plant Physiol. **51**, 848-851.

Poovaiah, B.W., Leopold, A.C. (1973b). Deferral of leaf senescence with calcium. Plant Physiol. **52**, 236-239.

Richmond, T.A., Somerville, C.R. (2001). Integrative approaches to determining Csl function. Plant Mol. Biol. **47**, 131-143.

Robson, A.D., Pitman, M.G. (1983). Interactions between nutrients in higher plants. In Encyclopedia of Plant Physiology. Edited by lauchil, A. and Bieleskii, R.L. 147-180. Springer-Verlag, Berlin.

Sanders, D., Pelloux, J., Brownlee, C., Harper, J.F. (2002). Calcium at the crossroads of signaling. Plant Cell, S401-S417.

Scheible, W.R., Eshed, R., Richmond, T., Delmer, D., Somerville, C. (2001) Modifications of cellulose synthase confer resistance to isoxalen and thiazolidinone herbicides in *Arabidopsis Ixr*1 mutants. Proc. Natl. Acad. Sci. USA **98**, 10079-10084.

Seawright, A.A., Ng, JC, Oelrichs, PB, Sani, Y., Nolan C.C., Lister, A.T., Holton, J., Ray, D.E., Osborne R. (1999). Biology and conservation of cycads. Proceedings of the Fourth International Conference on Cycad Biology (Panzhihua, China).

Shure, M., S. Wessler, N. Fedoroff. (1983). Molecular identification and isolation of the waxy locus in Maize. Cell **35**, 225-233.

Spencer PS, Nunn PB, Hugon J, Ludolph AC, Ross SM, Roy DN, Robertson RC (1987) Guam amyotrophic lateral sclerosis-parkinsonism-dementia linked to a plant excitant neurotoxin. Science **237**, 517-522.

Sun, Y., Olson, R., Horning, M., Armstrong, N., Mayer, M., Gouaux, E. (2002). Mechanism of glutamate receptor desensitization. Nature **417**, 242-253.

Szatkowski, M., Attwell, D. (1994). Triggering and execution of neuronal death in brain ischaemia: two phases of glutamate release by different mechanisms, Trends Neurosci. **17**, 359-365.

Thion, L., Mazars, C., Nacry, P., Bouchez, D., Moreau, M., Ranjeva, R., Thuleau, P. (1998). Plasma membrane depolarization-activated calcium channels, stimulated by microtubule depolymerizing drugs in wild-type *Arabidopsis thaliana* protoplasts, display constitutively large activities and a longer half-life in *ton* 2 mutant cells affected in the organization of cortical micotubules. Plant J. **13**, 603-610.

Vega A, Bell, E.A. (1967). α-Amino-β-methylaminopropionic acid, a new amino acid from seeds of *Cycas circinalis*. Phytochem. **6**, 759-762.

Véry, A-A., Sentenac, H. (2003). Molecular mechanisms and regulation of K^+ transport in higher plants. Annu. Rev. Plant Biol. **54**, 575-603.

Von Arnim, D., Deng, X-W. (1996). Light control of seedling development. Annu. Rev. Plant Physiol. Plant Mol. Biol. **47**, 215-243.

Vovides, A.P., K.J., Norstog, P.K., Fawcett, M.W., Duncan, R.J., Nash, D.V., Molsen. (1993). Histological changes during maturation in male and female cones of the cycad Zamia furfuracea and their significance in relation to pollination biology. Bot. J. Linnean Soc. **111**, 241-252.

Wei, N, Kwok, S.F, von Arnim, A.G. Lee, A., MacNellis, T.W, Piekos, B, Deng. X-W. (1994). *Arabidopsis COP*8, *COP*10 and *COP*11 genes are involved in repression of photomorphogenic developmental pathway in darkness. Plant Cell **6**, 629-643.

Weiss, J.H., Choi, D.W. (1988). Beta-*N*-methylamino-L-alanine neurotoxicity: requirement for bicarbonate as a cofactor. Science **241**, 973-975.

Weiss, J.H., Koh, J-Y, Choi, D.W. (1989). Neurotoxicity of B-N-methylamino-L-alanine (BMAA) and B-N-oxalylamino-L-alanine (BOAA) on cultured cortical neurons. Brain Research **497**, 64-71.

Weiss, J.H., Choi, D.W. (1991). Slow non-NMDA receptor mediated neurotoxicity and amyotrophic lateral sclerosis. Adv. Neurol. **56**, 311-328.

Whittaker, R.H., Feeny, P.P. (1971). Allelochemics: chemical interactions between species. Science **171**, 757-770.

Williams, J.H., Errington, M.L., Lynch, M.A., Bliss, T.V.P. (1989). Arachidonic acid induces a long-term activity-dependent enhancement of synaptic transmission in the hippocampus. Nature **341**, 739-742.

Wilson, J.M.B., Khabazian, I., Wong, M.C., Seyedalikhani, A., Bains, J.S., Pasqualotto, B.A., Williams, D.E., Andersen, R.J., Simpson, R.J., Smith, R., Craig, U-K., Kurland, L.T., Shaw, C.A. (2002). Behavioral and neurological correlats of ALS-Parkinsonism Dementia complex in adult mice fed washed cycad flour. NeuroMolecular Medicine **1**, 207-222.

Wisden, W., Seeburg, P.H. (1993). Mammalian ionotropic glutamate receptors. Curr. Opin. Neurobiol. **3**, 291-298.

Wymer, C.L., Bibikova, T.N., Gilroy, S. (1997). Cytoplasmic free calcium distributions during the development of root hairs of *Arabidopsis thaliana*. Plant J. **12**, 427-439.

Zhang, H., Hanley, S., Goodman, H.M. (1991). Isolation characterization and chromosomal location of a new cab gene from *Arabidopsis thaliana*. Plant Physiol. **96**, 1387-1388.

Zhong, R., Kays, S.J., Schroeder, B.P., Ye, Z.-H. (2002). Mutation of a chitinase-like gene causes ectopic deposition of lignin, aberrant cell shapes, and overproduction of ethylene. Plant Cell **14**, 165-179.